

# **Tropospheric Radio Duct Meteorology at VHF and UHF in Theory and as Observed on a Trip Around the World, February 8 to March 15, 1962**

**D. L. RANDALL**

*Wave Propagation Branch  
Electronics Division*

**May 31, 1966**



**U.S. NAVAL RESEARCH LABORATORY  
Washington, D.C.**

**DISTRIBUTION OF THIS DOCUMENT IS UNLIMITED**

## CONTENTS

Abstract	iii
Problem Status	iii
Authorization	iii
<b>INTRODUCTION</b>	<b>1</b>
<b>THEORY</b>	<b>1</b>
<b>EXPERIMENTAL VERIFICATION</b>	<b>6</b>
Mission 1, McChord AFB, Washington, to Hickam AFB, Hawaii	7
Mission 2, Hickam AFB, Hawaii, to Tafuna, Samoa	11
Mission 3, Tafuna, Samoa, to Nandi, Fiji	16
Mission 4, Nandi, Fiji, to Sydney, Australia	16
Mission 5, Sydney, Australia, to Perth, Australia	19
Mission 6, Perth, Australia, Local Flight 1	26
Mission 7, Perth, Australia, Local Flight 2	29
Mission 8, Perth, Australia, Local Flight 3	33
Mission 9, Perth, Australia, to Singapore	34
Mission 10, Singapore to Bangkok, Thailand	38
Mission 11, Bangkok, Thailand, to Calcutta, India	42
Mission 12, Karachi, Pakistan, Local Flight	43
Mission 13A, Karachi, Pakistan, to Dhahran, Saudi Arabia, and Mission 13B, Dhahran, Saudi Arabia, to Nicosia, Cyprus	52
Mission 14, Nicosia, Cyprus, to Rota, Spain	56
Mission 15, West Malling, England, to Keflavik, Iceland	60
Mission 16, Keflavik, Iceland, to Patuxent NAS, Maryland	65
<b>CONCLUSIONS</b>	<b>70</b>
<b>WORLD DIVERGENCE MAPS</b>	<b>75</b>
<b>REFERENCES</b>	<b>77</b>

## ABSTRACT

Vorticity fields showing areas of divergence or convergence in the air-mass flow channels at or above the gradient wind level may be located on a weather map and are theoretically related to the formation or dissipation of elevated radio ducts at vhf and uhf. Theoretical predictions of elevated radio duct formation have been verified by measurements made on a trip around the world, February 8 to March 15, 1962, in a Naval Research Laboratory aircraft. It was verified that ducts result from warm dry air subsiding over cooler moist air in a divergence (anticyclone) area during conditions of stable or increasing pressure. On the basis of the theory and the meteorological measurements, oceanic regions in the world most likely to support radio duct formation at different seasons of the year were mapped. For either the Northern or the Southern Hemisphere, in winter these regions are predominantly in the Torrid Zone but in summer have extended farther into the Temperate Zone and are less prevalent in the Torrid Zone.

## PROBLEM STATUS

This is an interim report on a continuing problem.

## AUTHORIZATION

NRL Problem R07-05  
Project RR 008-01-41-5553

Manuscript submitted March 7, 1966.

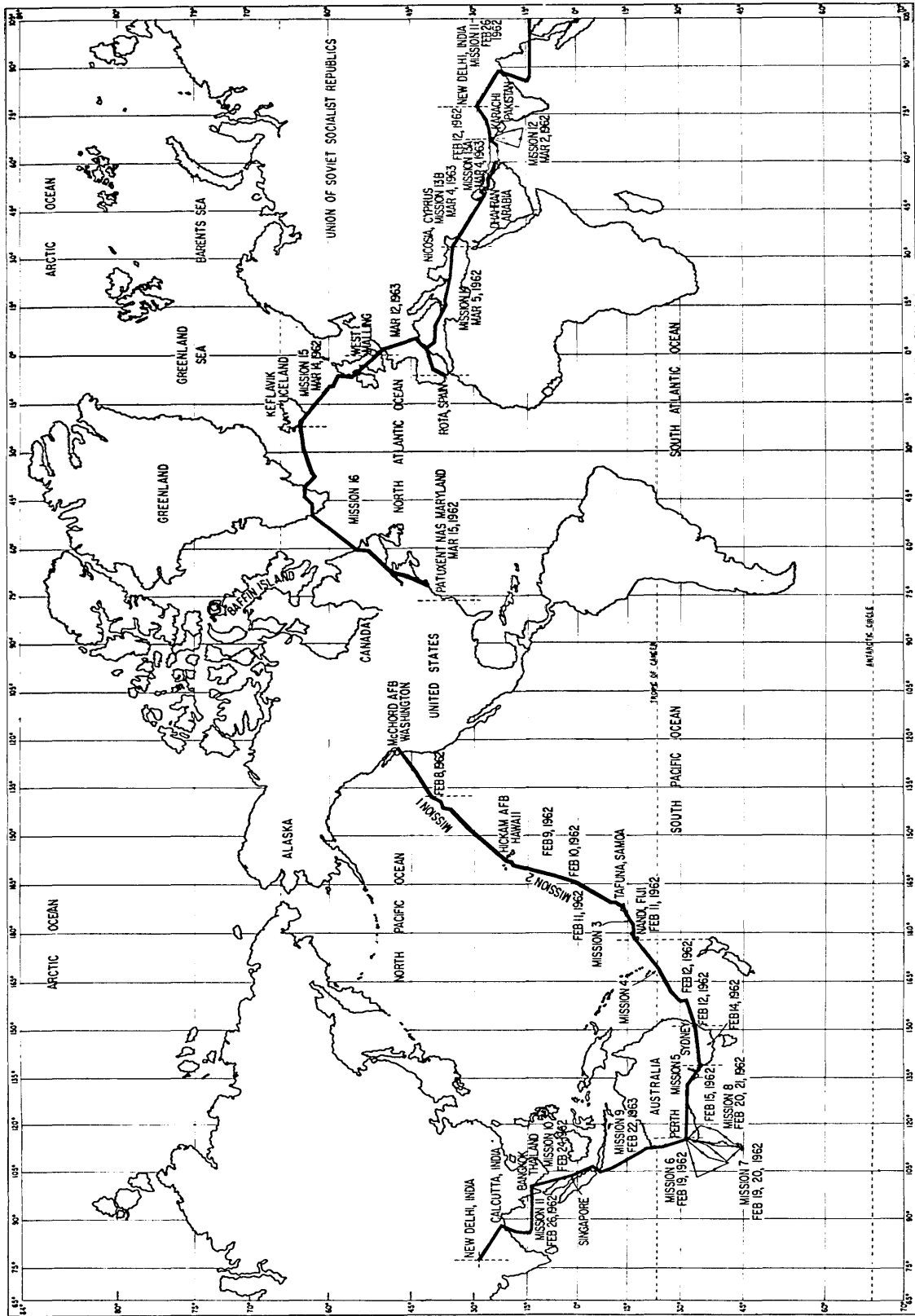


Fig. 1 - Missions flown on a trip around the world

# TROPOSPHERIC RADIO DUCT METEOROLOGY AT VHF AND UHF IN THEORY AND AS OBSERVED ON A TRIP AROUND THE WORLD, FEBRUARY 8 TO MARCH 15, 1962

## INTRODUCTION

It has long been known that, in certain regions of the world (1-4), vhf and uhf radio transmission can take place over much longer distances than would otherwise be expected. This anomalous propagation was soon found to take place in ducts which seemed to appear in a fairly consistent manner, depending on weather conditions. If the proper weather conditions could be identified and, better yet, predicted, vhf and uhf radio communications systems all over the world would be greatly benefitted.

We now have a reasonable explanation for the formation of some of these radio ducts, but it is necessary to correlate the theoretically predicted regions of radio duct formation with those which actually occur. Therefore we undertook to compare the predicted locations of radio ducts with meteorological maps and radio soundings made on a round-the-world trip during February and March 1962 (Fig. 1). Before the results of this flight are discussed, it will be helpful to review some of the basic meteorological considerations of tropospheric radio-wave propagation.

Thus the purpose of this report is to apply the equations developed in the next section to the radio meteorological data observed by the Naval Research Laboratory Flying Laboratory (Aircraft 128-324) while making a trip around the world from February 8 to March 15, 1962, and to suggest a system of radio duct predication based on the data measured.

## THEORY

There are several distinct layers in the atmosphere over the ocean. The lowest, known as the marine layer, is relatively moist and is subject to the frictional force of the rotating earth and to surface heating; this moist air has a relatively high refractive index. Above the marine layer is the gradient wind layer, where the wind flow is in equilibrium with the pressure gradient force, the centrifugal force, and the Coriolis force. Tropospheric radio ducts, as defined here, are due to large-scale air-mass currents, above the gradient layer, which produce dry-air layers with relatively low refractive indexes descending over the relatively moist marine layer. This moisture discontinuity is stabilized by a temperature inversion layer, with a warmer layer of dry air subsiding over a usually turbulent, colder, moister marine layer. The motions of these air masses produce a region that acts as an atmospheric waveguide for vhf and uhf radio waves. That is, a region of steeply negative refractive index gradient (or dielectric constant gradient) is sandwiched between two regions of moderately negative refractive index gradient (with the lower layer having the higher average value), and the steeply negative gradient bends the rays of the radio waves more sharply than the earth's curvature.

The air currents which produce this situation may be described in terms of their vorticity and the factors which determine refractive index, namely, pressure, temperature, and humidity. Two equations, based on vorticity theory (5), will be used to describe the air-parcel motions above the interface of moist and dry air which usually forms radio ducts.

In most meteorological studies it is convenient to consider surfaces of constant energy, which are both isentropic and isenthalpic. These surfaces are characterized by a unique potential temperature, which is the temperature a parcel of air would have at that energy if it were dry and adiabatically compressed to a pressure of 1000 millibars. Let us consider a particular parcel of dry air moving along a streamline above the marine layer. Vorticity theory states that the product of the vertical component of the absolute vorticity  $\zeta_a$  and the horizontal area  $A$  of the fluid air parcel is a constant  $k$  :

$$A \zeta_a = k . \quad (1)$$

This relation can be expressed in another form by measuring the pressure differential  $d\rho$  between two potential temperature surfaces that are a temperature differential  $d\theta$  apart, so that

$$(d\theta/d\rho) \zeta_a = k' . \quad (1')$$

By differentiating Eq. (1) with respect to time one obtains

$$-(1/\zeta_a)(d\zeta_a/dt) = (1/A)(dA/dt) = D, \quad (2)$$

where  $D$  is called divergence if the percentage rate of change of area with respect to time is positive.

The absolute vorticity  $\zeta_a$  is equal to the relative vorticity  $\zeta_r$  plus the Coriolis parameter  $f$ , which is twice the component of the earth's angular velocity normal to the surface at a given latitude. Thus

$$\zeta_a = \zeta_r + f . \quad (3)$$

The relative vorticity can be measured on a weather map and is given by

$$\zeta_r = V/R + dV/dh, \quad (4)$$

where  $V$  is the velocity at the gradient wind level,  $R$  is the radius of curvature of the isobar, and  $h$  is the distance along the normal between two isobars. The term  $dV/dh$  is a measure of the shear in the air stream.

Equation (2) may be written in the form

$$-\dot{\zeta}_a/\zeta_a = D$$

which, after introduction of Eq. (3), becomes

$$\dot{\zeta}_r = -D\zeta_a - \dot{f} .$$

Since (Fig. 2)  $f = 2\Omega \sin \phi$ , where  $\Omega$  is earth's angular velocity and  $\phi$  is the latitude,\*

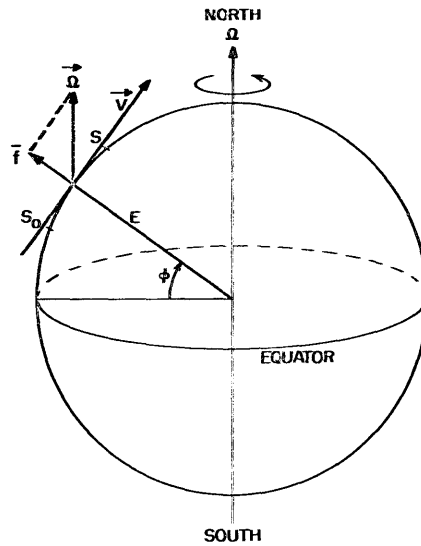
$$\dot{\zeta}_r = -D\zeta_a - 2\Omega (\cos \phi) \dot{\phi}$$

and since  $E\dot{\phi} = v$ , where  $E$  is the mean radius of the earth and  $v$  is the northward wind velocity,

$$\dot{\zeta}_r = -D\zeta_a - 2\Omega (\cos \phi)v/E .$$

\*See Ref. 6, page 132, for an explanation of the factor 2.

Fig. 2 - Parameters used in the meridional flow equation



If  $2\Omega (\cos \phi)/E$  is defined as  $\beta$ , this becomes

$$\dot{\zeta}_r = -D \zeta_a - \beta v. \quad (5)$$

We will now consider the wind flow along a meridian. For straight isobars in a broad shearless flow channel,  $\dot{\zeta}_r$  and  $\zeta_r = 0$ . Then  $-D\zeta_a = \beta v$ ; but also  $D = -\dot{\zeta}_a/\zeta_a$ . It follows that

$$-(\dot{\zeta}_a/\zeta_a)\zeta_a = \beta v \text{ or } \dot{\zeta}_a = \beta v. \quad (6)$$

Integrating Eq. (6) with respect to time we obtain (see Fig. 2)

$$\zeta_a - \zeta_{a_0} = \bar{\beta} (S - S_0), \quad (7)$$

where  $\bar{\beta}$  is defined as  $(2\Omega/E) \cos \bar{\phi}$ , and  $\bar{\phi}$  is the mean latitude of the path  $(S - S_0)$  along a meridian. If we now substitute the value of  $\zeta_a$  from Eq. (1') into Eq. (7), we obtain an equation relating pressure thickness between two potential temperature surfaces to latitude distance:

$$K'/(d\theta/dp) - K'/(d\theta/dp)_0 = \bar{\beta} (S - S_0)$$

or

$$(K'/(d\theta))(dp - dp_0) = \bar{\beta} (S - S_0). \quad (8)$$

Equation (8) states that for a parcel of dry air flowing in a channel at the gradient wind level the pressure differential of the parcel between two potential temperature surfaces (adiabatics)  $d\theta$  apart decreases as the parcel is displaced equatorward along a meridian (Fig. 3) the distance  $S - S_0$ .

When the pressure thickness between two potential temperature surfaces changes, it is obvious that the rate of change of temperature with height, or lapse rate of temperature, must change. For adiabatic meridional motions along an isobar, it can be shown (6) that

$$\zeta_a (G_d - G) = \zeta_{a_0} (G_d - G_0) \quad (9)$$

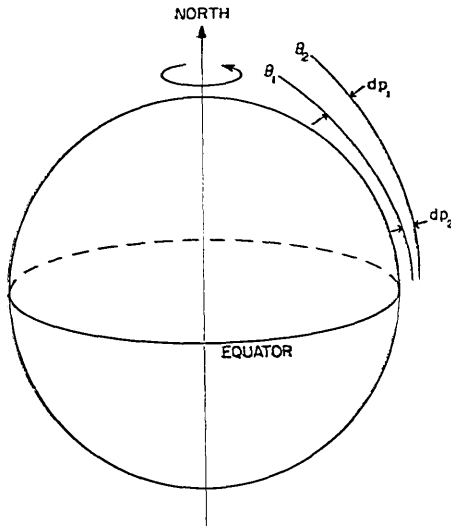


Fig. 3 - Variation of pressure differential between two potential temperature surfaces with latitude

where  $G_d$  is the dry adiabatic temperature lapse rate,  $G_o$  is the lapse rate in a given parcel when its vorticity is  $\zeta_{a_0}$ , and  $G$  is the lapse rate in the given parcel when its vorticity is  $\zeta_a$ . If a given point has vorticity  $\zeta_{a_0}$  and lapse rate  $G_o$ , this equation means that the vorticity  $\zeta_a$  will decrease and the lapse rate  $G$  will increase. In this case decreasing  $\zeta_{a_0}$  will produce the condition of divergence. At the center of an anticyclone, where divergence exists, one would expect a steeper lapse rate of temperature than in a cyclone where convergence exists. This formula holds only for the dry adiabatic case and frequently fails in the convergent conditions of cyclones.

At the center of an anticyclone above the ocean, or its associated ridge of high pressure, air tends to flow outward. To maintain this flow air must be subsiding from aloft. An indication of this subsidence is the increase in pressure at the center; hence the pressure differential between two potential temperature surfaces decreases, since the air parcels are being adiabatically compressed. On the other hand, in the center of a cyclone, or its associated low-pressure trough, the air tends to flow inward, and there is a rising column of air at the center. In this case there is a decrease in pressure at the center with respect to time; there is convergence, and the pressure differential between potential temperature surfaces increases.

Conditions are now ripe for the formation or dissipation of radio ducts. Owing to horizontal divergence in the warm dry air, parcels subside and are compressed adiabatically, with the result that the temperature lapse rate in these parcels steepens. In the marine layer parcels are caused to rise vertically from frictional turbulence or surface heating. As these parcels rise they are cooled adiabatically, and their temperature lapse rate decreases until they reach the warm descending parcels. A strong temperature inversion layer then results. The vertical motion of the colder air parcels from the surface is checked because, as soon as they reach the warm air above they are relatively more dense than their environment; hence they sink to a level of density equilibrium. This condition creates a sharp moisture discontinuity, and the moisture-laden parcels spread out horizontally at the temperature inversion layer. This can be seen visually as a stratus cloud or haze layer. From the equation for the refractive index gradient, which becomes (7)

$$dN/dh = \text{Const.} - 0.89 dT/dh + 4.14 de/dh \quad (10)$$

when the pressure  $p$  is 1000 millibars, the temperature  $T$  is 300°K, and the water vapor pressure  $e$  is 10 millibars, we can now see that we have the negative refractive index

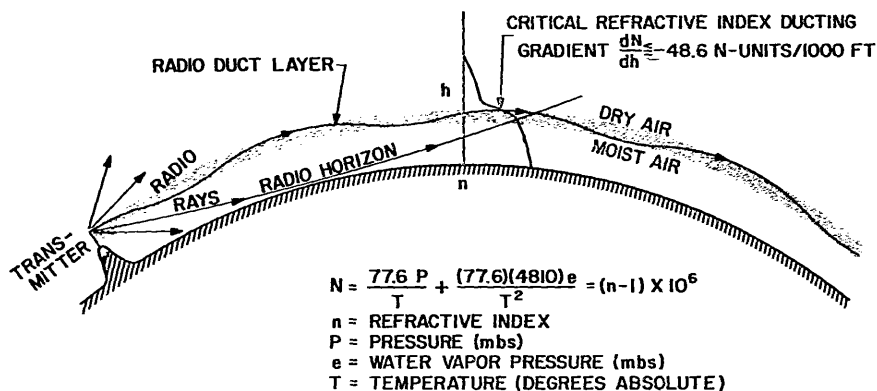


Fig. 4 - Anomalous propagation through a radio duct layer

gradient that bends rays of radio waves downward; there is both a discontinuous temperature increase ( $dT/dh$  large and positive) and a moisture drop ( $de/dh$  large and negative) within the duct layer. When horizontally propagated vhf and uhf rays are bent with a curvature greater than that of the surface of the earth, a radio duct is said to exist (Fig. 4). This critical gradient is about  $-48.6$  N-units/1000 feet.

The values for these equations, which may be read from a weather map and a meteorological sounding, determine the density changes in the dry air parcel at or above the gradient wind level. In order to relate the values for these equations to the problem of radio duct propagation, it is first necessary to show that radio duct formation is taking place in a certain region; then these values may be used to predict radio duct formation at a later time. Equation (8) specifies initial and final conditions. If the duct is present initially, and the equation predicts divergence downstream, then duct continuation may be expected downstream. On the other hand, if the equation predicts convergence, and a duct is not initially present, duct formation would not be expected. If the conditions of Eq. (9) predict duct formation initially, and if the lapse rate either remains constant or increases, then duct formation may be expected in the final condition. At the center of an anticyclone, if conditions are right for the existence of a radio duct, and the subsidence process continues as indicated by rising pressure tendencies, then the radio duct will persist. At the center of a cyclone, if a radio duct does not already exist and the air column continues to rise from convergence as indicated by falling pressure tendencies, then a radio duct will not be formed so long as the convergence continues.

In describing the convergence and divergence process taking place we have visualized the thickening or thinning of the layer of air between two potential temperature surfaces (Eq. (8)). The potential temperature is used because it is a conservative property of an air mass and acts as a tag on an air parcel. Another quantity which acts as an air parcel tag, or conservative property, is the specific humidity  $q$ . It is defined as the ratio of the water vapor density to the total air density. If the parcel is raised up or down, this ratio remains constant so long as moisture is not added or subtracted. The specific humidity can also be expressed as  $q = 0.622 e/P$  where  $e$  is the water vapor pressure and  $P$  is the total pressure.

With these two air parcel tags (8) it is possible to track air masses as they move over the face of the earth. An air mass at a source region over tropical waters becomes moist and warm. Typical values of specific humidity may vary from 16 to 23 grams per kilogram, and typical values of potential temperature from 300 to 310 degrees Kelvin. An air mass having its origin over tropical waters is called a maritime tropical air mass and designated mT. An air mass having its source region over temperate zone waters is

designated as a maritime polar air mass, mP, and may have values of specific humidity from 4 to 10 grams per kilogram and potential temperatures from 280 to 298 degrees Kelvin. Air masses originating in polar regions, whether they originate over land or water, are very similar, because frozen ice is much the same whether it is on land or water. Continental polar air masses, cP, have the lowest values of specific humidity, from about 1.0 to 4.0 grams per kilogram, and potential temperature from about 270 to 278 degrees Kelvin. When an air mass leaves its source region it is constantly undergoing change, and it is difficult to say when an air mass changes from one type to another; however when frontal zones are encountered, or air trajectories are considered, this classification system is very useful.

#### EXPERIMENTAL VERIFICATION

The missions flown (Fig. 1) on this trip by the NRL Flying Laboratory were the following:

<u>Mission Number</u>	<u>Points of Departure and Arrival</u>	<u>Date</u>
1	McChord AFB, Washington, to Hickam AFB, Hawaii	Feb. 8-9
2	Hickam AFB, Hawaii, to Tafuna, Samoa	Feb. 10-11
3	Tafuna, Samoa, to Nandi, Fiji	Feb. 12
4	Nandi, Fiji, to Sydney, Australia	Feb. 12
5	Sydney, Australia, to Perth, Australia	Feb. 13-14
6	Perth, Australia, local flight 1	Feb. 19
7	Perth, Australia, local flight 2	Feb. 19-20
8	Perth, Australia, local flight 3	Feb. 21
9	Perth, Australia, to Singapore	Feb. 22
10	Singapore to Bangkok, Thailand	Feb. 24
11	Bangkok, Thailand, to Calcutta, India	Feb. 26
12	Karachi, Pakistan, local flight	Mar. 2
13A	Karachi, Pakistan, to Dhahran, Arabia	Mar. 3
13B	Dhahran, Arabia, to Nicosia, Cyprus	Mar. 4
14	Nicosia, Cyprus, to Rota, Spain	Mar. 5
15	West Malling, England, to Keflavik, Iceland	Mar. 14
16	Keflavik, Iceland, to Patuxent NAS, Maryland	Mar. 15

On this trip around the world soundings of refractive index and temperature vs pressure-height were made at the beginning and end of each flight, and if possible during the missions. Visual observations of clouds and visibility were made throughout the trip. Whenever possible cloud pictures were made by a time-lapse camera mounted in the cockpit of the aircraft. In addition surface weather maps and radiosonde observation were obtained for each mission.

In discussion of these flights we will assume the following arbitrary definitions: A sounding is a measurement of temperature, pressure, and refractive index in which the aircraft makes an altitude change of 1000 feet or more. The ascensional rate is

usually 500 feet per minute, although it may be less. A probe is an aircraft measurement of temperature, pressure, and refractive index in which the change in altitude is less than 1000 feet but equal to or greater than 100 feet. Changes in altitude of less than 100 feet are not considered in computing gradients of refractive index and temperature because the horizontal speed of the aircraft is usually 25 to 60 times greater than the vertical speed. Furthermore, the ability to read pressure height changes of less than 100 feet on the Viscorder is questionable.

A radio duct will be assumed if a layer is 100 nautical miles or more in length and has a refractive index gradient equal to or more negative than  $-48.6$  N-units/1000 feet. It is also assumed that an N-break of 15 N-units or more is necessary. It is impractical to make vertical soundings of refractive index every 100 nautical miles over a propagation path, but it has been observed that if a sounding is made down through the dry air into a stratus and/or haze layer, which can visually be seen to be continuous (2,3), then the refractive index gradient is also continuous at this dry-moist interface. The existence of a radio duct is demonstrated by the propagation of vhf or uhf signals along the interface of dry air and the cloud and/or haze layer to distances greater than the radio horizon. For these measurements the aircraft is flown at the dry/moist air interface. During these flights it was not always possible to use the vhf equipment for verification of a radio duct, so there were times when ducts were assumed to exist from meteorological conditions without verification by radio reception.

The conditions for no radio duct would be the absence of any of those mentioned above. There were times when a refractive index gradient of  $-48.6$  N-units/1000 feet or less was observed, but the cloud layer was not continuous for 100 nautical miles or more. This condition often occurred in convective-type clouds which penetrated the layer in which the duct was being followed by the aircraft. If convective penetration of the dry/moist air interface was prevalent over an extensive area of 100 nautical miles or more, the radio duct was assumed to be lost.

Mission 1, McChord AFB, Washington,  
to Hickam AFB, Hawaii

The first 860 nautical miles of the trip from McChord AFB to Hickam AFB was in a current of air with a general southerly component of motion aloft, and the remaining 1513 nautical miles was in a current of air having a northerly component of motion (Fig. 5). In general, then, for air parcels carried in the southerly current the absolute vorticity should be increasing (Eq. (7)), the lapse rate should be increasingly unstable (Eq. (9)), and there should be convergence (Eq. (2)). This is not a favorable condition for radio duct formation at vhf and uhf.

On the other hand, in the northerly current of air the absolute vorticity should be decreasing (Eq. (7)), the lapse rate should be increasingly stable (Eq. (9)), and there should be increasing divergence (Eq. (2)). Since conditions are favorable for radio duct formation in the subsiding air associated with horizontal divergence, decreasing absolute vorticity, and increasingly stable lapse rates of temperature, there should be more favorable conditions for radio duct formation in the latter portion of the flight.

In the first 860 nautical miles the flight path crossed three occluded fronts (Figs. 5 and 6). The conditions of unstable lapse rate as indicated were evidenced by the cloud banks of unknown tops and the rain encountered while crossing the fronts.

As would be expected from Eqs. (9) and (2) the lapse rate tended to be unstable in the current of air moving from south to north. The Seattle radiosonde (Fig. 6) shows a dry dry adiabatic lapse rate from 2000 to 5000 feet and a near moist adiabatic lapse rate from 5000 to 10,000 feet. This is what would be expected with the turbulence and rain



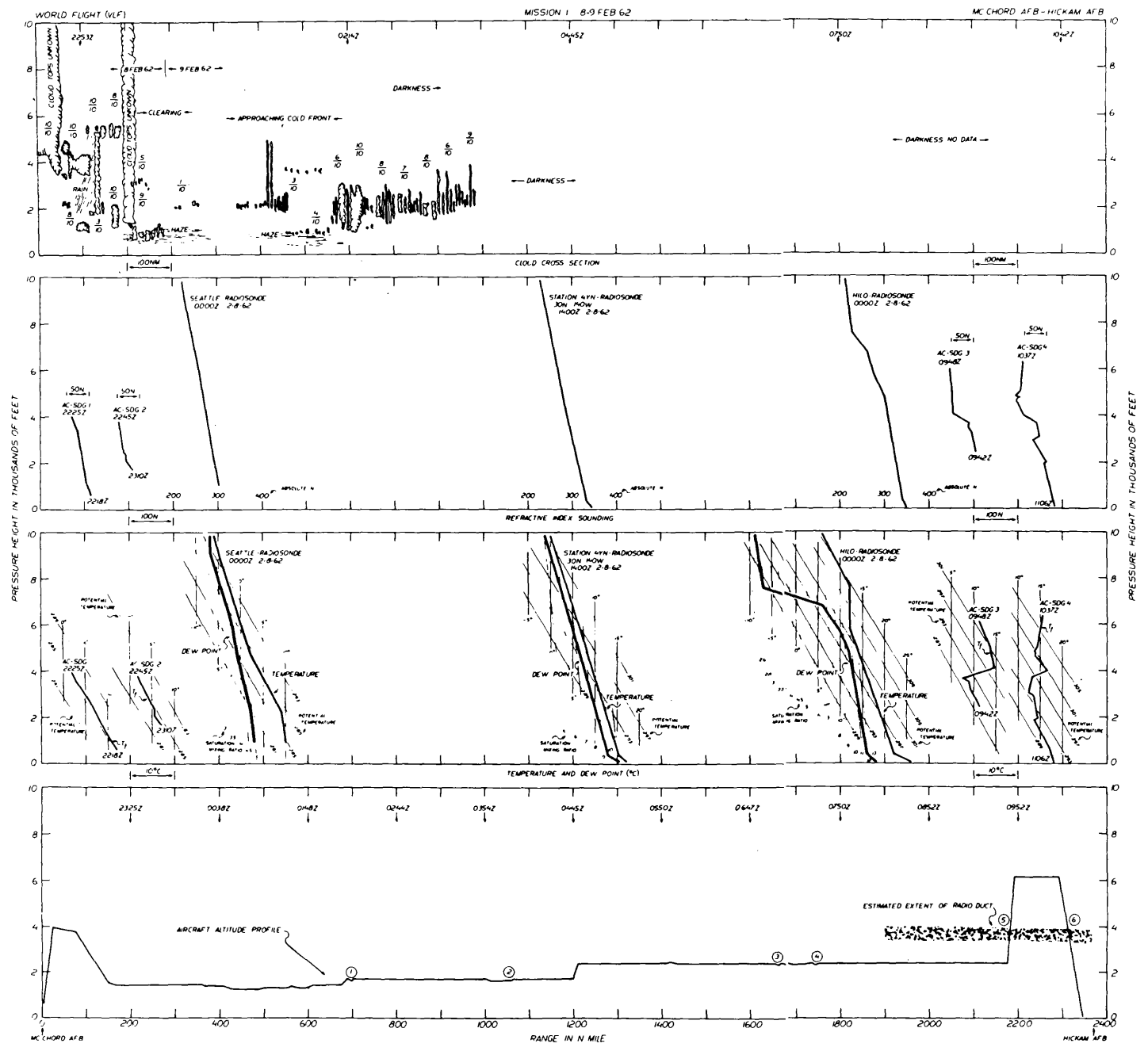


Fig. 6 - Cross section of meteorological conditions from McChord AFB, Washington, to Hickam AFB, Hawaii (Mission 1)

Table 1  
Summary of Mission 1

Position Number	Sounding or Probe	N-break (N-units)	dN/1000	Layer		Temperature		dT/1000 (ft)	Layer		Distance (naut mi)	Time (Z)
				Top (ft)	Base (ft)	Top (°C)	Base (°C)		Top (ft)	Base (ft)		
1	Probe	15	--	1700	1650	9.3	8.6		1700	1650	698	0213
2	Probe	18	--	1700	1650	8.9	8.7	+ 4.0	1700	1650	1060	0410
3	Probe	16	--	2400	2350	8.9	8.6	+ 6.0	2400	2350	1666	0707
4	Probe	15	--	2400	2350	9.0	9.4		2400	2350	1738	0730
5	Sounding	35	-78	4100	3650	14.6	7.5	+15.8	4100	3650	2185	0940
6	Sounding	28	-93	4000	3700	16.5	13.0	+11.7	4000	3700	2310	1047

Table 2  
Refractive Index Gradients

Seattle, Washington, 00Z, Feb. 8, 1962		Station 4YN, 14Z, Feb. 8, 1962		Hilo, Hawaii, 00Z, Feb. 8, 1962	
Layer (10 <sup>3</sup> ft)	dN/dh	Layer (10 <sup>3</sup> ft)	dN/dh	Layer (10 <sup>3</sup> ft)	dN/dh
9.9 to 9.1	- 5	9.9 to 4.8	- 6	9.9 to 7.5	- 5
9.1 to 4.8	-10	4.8 to 0.4	-10	7.5 to 6.7	-40
4.8 to 4.0	-10	0.4 to 0.1	-75	6.7 to 5.7	-30
4.0 to 2.2	-10			5.7 to 4.8	-20
2.2 to 0.9	-12			4.8 to 3.5	-12
				3.5 to 0.0	-26

Table 1 confirms the predictions of Eqs. (7), (8), and (9) by showing no radio duct formation in the first 1741 miles of the path. Although there were refractive index breaks of 15, 18, 16, and 15 N-units at points 1, 2, 3, and 4 respectively of Table 1 (and Fig. 6), the altitude change was 100 feet or less, which is indicative of a variation in horizontal homogeneity rather than in vertical structure. Points 5 and 6 show refractive index breaks of -78 and -93 N-units/1000 feet respectively. Aircraft probings at positions 1 through 4 showed no refractive index breaks (Fig. 6). The radiosonde observations (Table 2) showed no refractive index gradients less than -48.6 N-units/1000 feet, but the aircraft soundings at points 5 and 6 did. This is because the aircraft soundings were made nearly 10 hours after the radiosonde observation at Hilo, Hawaii, and the tendency toward increasing subsidence as predicted by Eqs. (2), (8), and (9) became effective.

On the basis of this increasing subsidence, and the observation of refractive index gradients in aircraft soundings at positions 5 and 6 the last 500 nautical miles of the flight was estimated to support radio duct formation conditions at vhf and uhf. This means that radio duct conditions existed during about one-fifth of the 2350 nautical miles flown on this mission.

Mission 2, Hickam AFB, Hawaii, to Tafuna, Samoa

Mission 2 is cited as an example of meridional flow in which divergence took place over most of the flight path (Figs. 7 and 8). The flow channel of maritime polar air is between the 1020 and 1015 isobar lines on the 155°W meridian, then curves south-southwestward following the winds toward Canton Island. The flow channel shows a

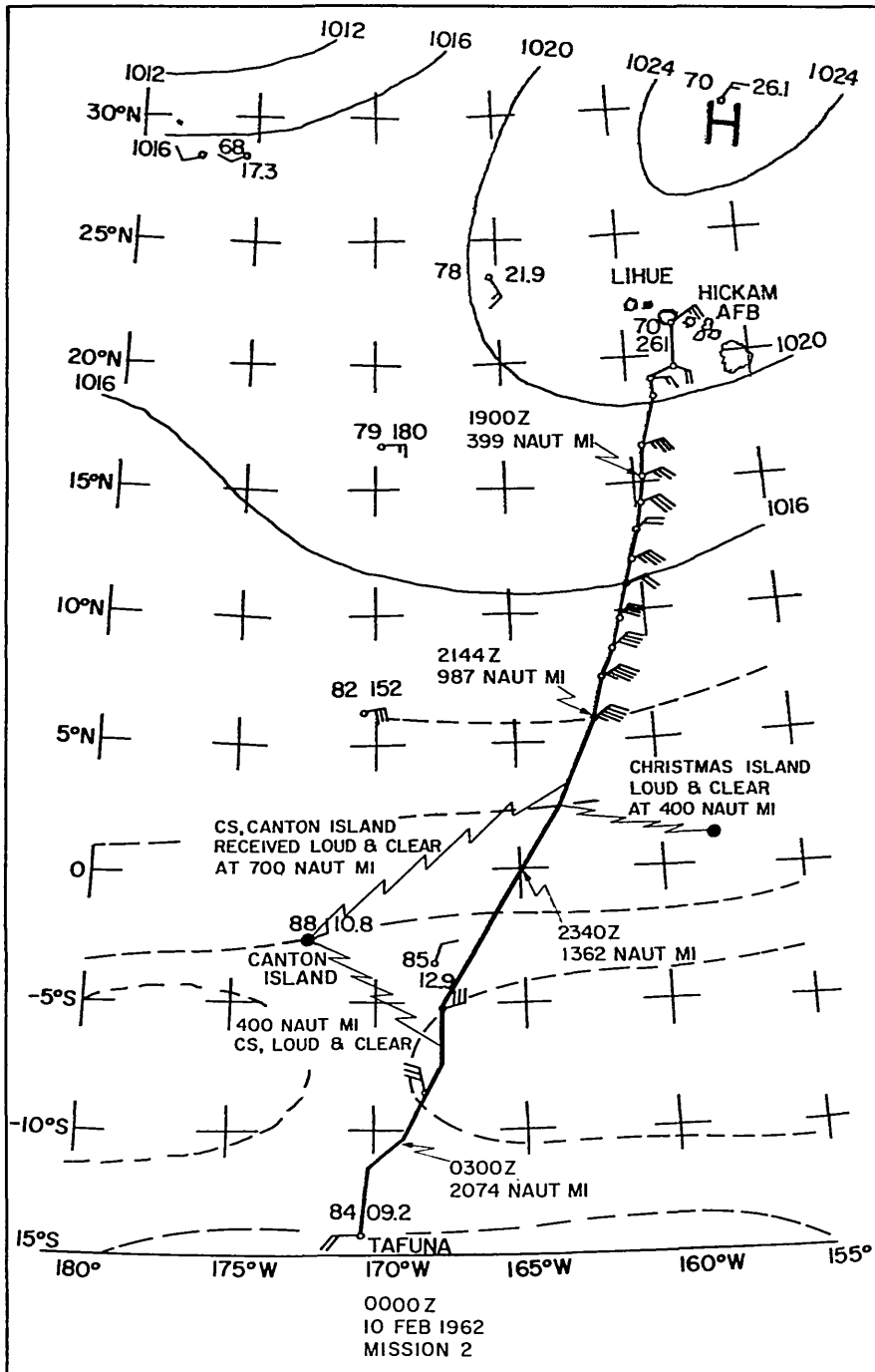


Fig. 7 - Sea-level pressure chart for the area between Hickam AFB, Hawaii, and Tafuna, Samoa (Mission 2)

component of velocity less than  $30^\circ$  parallel to the meridian. The flight path intersects the meridian at about  $15^\circ$  and crosses the main stream of the flow channel at about  $15^\circ$ . Although the flight path and the flow channel should be parallel, the conditions of Eq. (8) were met well enough to apply the formula, because the radiosonde and flight observations showed that the air mass was homogeneous. The radiosonde observation at Lihue, Hawaii, shows a refractive index gradient of  $-50$  N-units/1000 feet between 4450 to 5100 feet, and

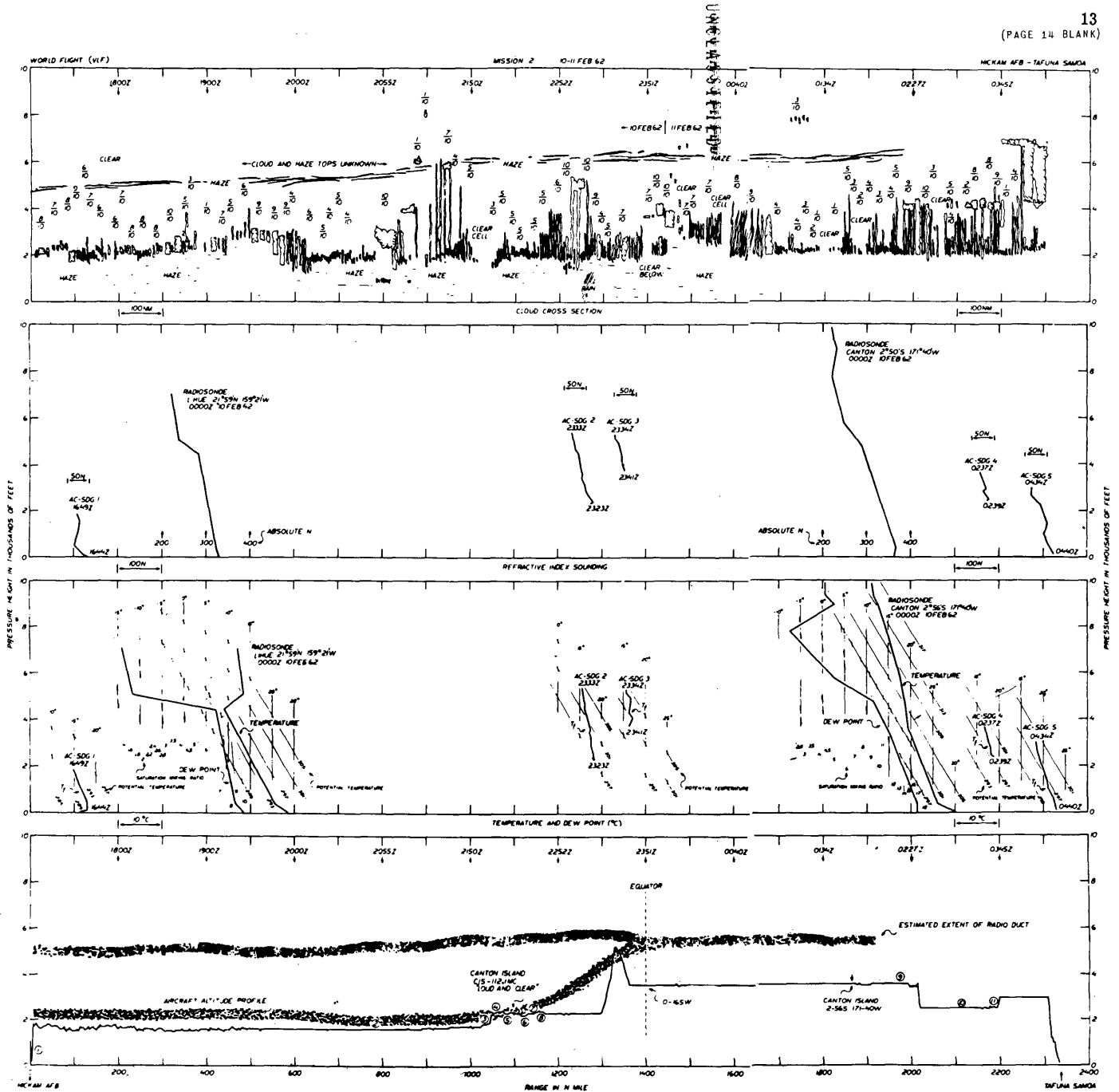


Fig. 8 - Cross section of meteorological conditions from Hickam AFB, Hawaii, to Tafuna, Samoa (Mission 2)

at Canton Island,  $3^{\circ}\text{S}$ , a refractive index gradient of  $-48$  N-units/1000 feet from 4800 to 5700 feet. The flight profile of the plane did not get high enough to measure this layer, which was shown by the radiosonde observations. The refractive index gradients, temperature gradients, and clouds indicated a second duct-layer ranging from 2000 to 4000 feet. This layer was pierced by convective clouds in several places. The reception of vhf radio signals from Canton Island more than 800 nautical miles from the aircraft (Fig. 8) is further evidence of the radio duct.

The Lihue, Hawaii, radiosonde observation 00Z, February 10, 1962 (Fig. 8), is typical of the air mass around the Hawaiian Islands, and it shows increased horizontal divergence (subsidence) over that indicated for the same region by the Hilo, Hawaii, sounding 00Z, February 8, 1962 (Fig. 6), because the top of the temperature inversion sank from 7000 feet to 5000 feet. Since the wind observations taken aboard the aircraft in this air mass have a pronounced north-to-south component, Eqs. (7) would indicate that this widespread area of horizontal divergence (subsidence) should increase in the air mass parcels as long as they have a northerly component of velocity. At the equator the Coriolis parameter in the absolute vorticity term of Eq. (2) becomes zero and then changes sign as the current of air moves southward across the equator. In this case divergence and convergence may be described by wind vectors. After crossing the equator the horizontal divergence decreases, and the subsiding layer tends to break up if the current of air is still moving from north to south.

That this layer of subsidence extended through the equatorial region is confirmed by radio reception from stations well beyond the radio horizon (Figs. 7 and 8). When the aircraft was at  $4^{\circ} 20'\text{N}$  and  $162^{\circ}40'\text{W}$  radio signals (112.1 Mc) were received "loud and clear" from south of the equator at Canton Island 700 nautical miles away. A short time later when the aircraft was at  $1^{\circ}30'\text{N}$  and  $164^{\circ}20'\text{W}$  radio signals (126.2 Mc) were picked up from Christmas Island more than 400 nautical miles away. Although the VOR navigation receiver was not monitored continuously, Canton Island was again received when the aircraft was at  $7^{\circ}00'\text{S}$  and  $168^{\circ}00'\text{W}$ . At this position the aircraft was about 400 nautical miles from the transmitter.

It is remarkable that this radio duct was pronounced enough that reception could be picked up beneath the layer. Previous examples of long-range ducting reception show the receiving aircraft in the radio duct (4).

The Canton Island radiosonde observation (Fig. 8), 00Z, February 10, 1962, shows that there is a tendency toward a radio duct layer, with a refractive index gradient of about  $-40$  N-units/1000 feet, but since this station is  $2^{\circ}50'$  south of the equator, a northward flowing stream of air parcels would not show a tendency toward increasing horizontal divergence (subsidence) as they would north of the equator. In the last 450 nautical miles of the path no more vhf signals were heard, and upon approaching Tafuna, Samoa, tremendous cumulonimbus clouds had formed. This strong convective activity should destroy a radio duct layer.

In Table 3, positions 3, 4, 5, 6, and 7 (Fig. 8) show refractive index gradients suitable for radio duct formation. It was in this area that the vhf signals from Canton Island and Christmas Island were first heard. At positions 8, 9, and 10 the altitude change of the flight probe was insufficient to compute a refractive index gradient. At position 11 a refractive index gradient of  $-240$  N-units/1000 feet was observed over an altitude change of 100 feet in a cumulus cloud formation. The temperature gradients at positions 3, 4, 5, 6, and 7 were all positive, which in general shows subsidence. This is in agreement with the other indication of subsidence and divergence noted. At position 11 the cloud layer was less than 100 nautical miles and the probe only 100 ft. In this case subsidence is not indicated.

Table 3  
Summary of Mission 2

Position Number	Sounding or Probe	N-break (N-units)	dN 1000 ft	Layer		Temperature		dT 1000 ft	Layer		Distance (naut mi)	Time (Z)
				Top (ft)	Base (ft)	Top (°C)	Base (°C)		Top (ft)	Base (ft)		
1	Sounding	32	- 64	500	0	17.8	16.0	+3.6	500	0	0	1644
2	Probe	16	--	1700	--	18.8	--	--	1700	--	780	2050
3	Probe	36	-144	2100	1850	20.0	19.3	+2.8	2100	1850	1045	2203
4	Probe	27	-270	2450	2350	19.0	18.8	+2.0	2450	2350	1066	2210
5	Probe	22	-220	2400	2300	18.9	18.8	+1.0	2400	2300	1080	2214
6	Probe	15	-150	2300	2200	19.3	18.8	+5.0	2300	2200	1125	2228
7	Probe	29	-290	2300	2200	19.0	18.5	+5.0	2300	2200	1145	2230
8	Probe	19	--	2500	--	17.8	--	--	2500	--	1155	2238
9	Probe	15	--	3650	--	16.7	--	--	3650	--	1975	0222
10	Probe	30	--	2600	--	20.0	--	--	2600	--	2065	0257
11	Probe	24	-240	2500	2400	19.4	19.0	+4.0	2500	2400	2188	0339

Table 4  
Refractive Index Gradients

Lihue, Hawaii, 00Z, Feb. 10, 1962		Canton Island, 00Z, Feb. 10, 1962	
Layer (10 <sup>3</sup> ft)	dN/dh	Layer (10 <sup>3</sup> ft)	dN/dh
7.5 to 5.1	- 8	9.3 to 8.9	-20
5.1 to 4.45	-50	8.9 to 7.7	+ 1
4.45 to 0.35	- 5	7.7 to 5.7	-12
0.35 to 0.00	-47	5.7 to 4.8	-48
		4.8 to 3.6	-45
		3.6 to 0.4	-12
		0.4 to 0.0	-28

The extent of the refractive index radio duct layer was estimated to be from Hickam AFB, Hawaii, to a distance of 1900 nautical miles. It was believed to be above the flight path, because there seemed to be no distinct haze or cloud layer at the flight level. The radio duct layer is based upon the observed refractive index gradient at Lihue radiosonde observation (Table 4), the observation of divergence (subsidence) from the wind field and temperature gradients, and the reception of vhf radio signals. This means that about four-fifths of the 2350 nautical miles on this flight were flown under conditions of radio duct formation.

### Mission 3, Tafuna, Samoa to Nandi, Fiji

The 750 nautical miles (Fig. 9) from Tafuna to Nandi was in the same maritime polar air mass (mP) as indicated on the sounding for Nandi, 23Z, February 10, 1962. The Nandi sounding shows that considerable mixing has taken place, because the temperature lapse rate lies between the moist and dry adiabatic curves. The cloud diagram (Fig. 9) for this flight shows convective rain and cloud tops continuing above 10,000 feet. The cloud tops for the first 300 nautical miles of the flight are unknown. This mixing is the explanation for the lack of stratification shown in the Nandi sounding. This mixing process is transforming a maritime polar air mass to a maritime tropical air mass, since it increases the moisture content of the upper layers of the air mass. From now on this body of air will be called a maritime tropical air mass.

Table 5 shows small N-breaks ranging from 15 to 23 N-units and radio duct gradients for positions 1, 2, 4, 5, 6, 7, 8, and 9 (Fig. 9). However with the exception of positions 2, 3, and 6 the radio duct layers were only 100 feet thick, and all of them were quite discontinuous as shown by the cloud diagram and the estimated extent of duct diagram (Fig. 9). Considering all the radio duct layer segments it is estimated that about 150 of the 700 nautical miles flown on this mission, or about one-fifth of the mileage supported radio duct formation at vhf and uhf.

### Mission 4, Nandi, Fiji, to Sydney, Australia

The flight from Nandi to Sydney (Fig. 10) continues on in the same maritime tropical air mass as was traversed from Tafuna to Nandi. However, at about 300 nautical miles from Nandi the flight path crossed a wedge of high pressure (Fig. 11), and continued on

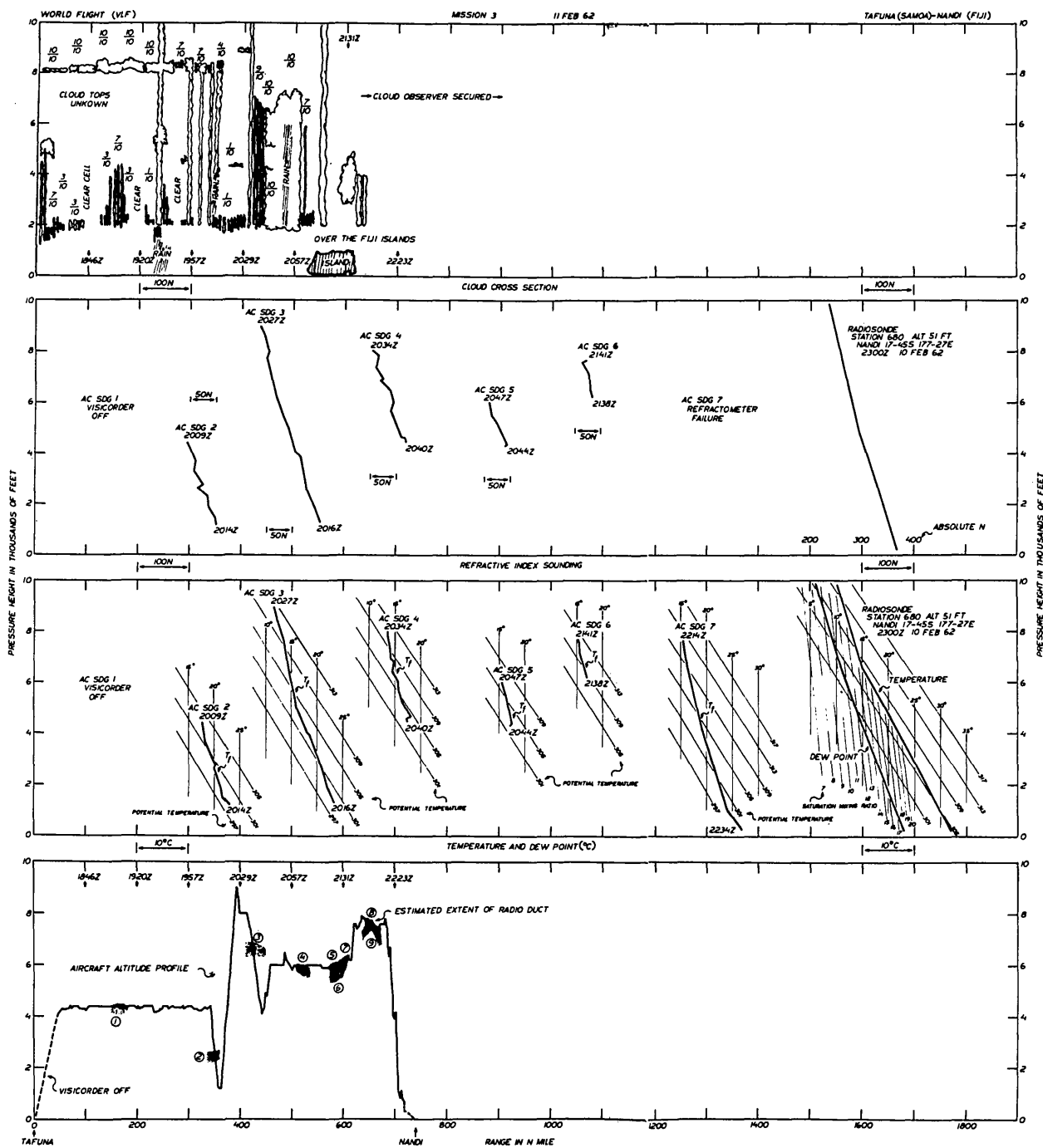


Fig. 9 - Cross section of meteorological conditions from Tafuna, Samoa, to Nandi, Fiji (Mission 3)



Table 5  
Summary of Mission 3

Position Number	Sounding or Probe	N-break (N-units)	dN 1000 ft	Layer		Temperature		dT 1000 ft	Layer		Distance (naut mi)	Time (Z)
				Top (ft)	Base (ft)	Top (°C)	Base (°C)		Top (ft)	Base (ft)		
1	Probe	15	-150	4500	4400	17.7	17.4	+ 3.0	4500	4400	161	1906
2	Sounding	17	-57	2650	2350	20.0	20.6	- 2.0	2650	2350	350	2012
3	Sounding	18	-45	6850	6450	14.8	14.5	+ 0.8	6850	6450	430	2038
4	Probe	16	-160	6000	5900	15.3	14.8	+ 5.0	6000	5900	473	2050
5	Probe	32	-320	6100	6000	16.4	17.1	- 7.0	6100	6000	580	2120
6	Probe	32	-128	6150	5900	18.1	17.5	+ 2.4	6150	5900	592	2126
7	Probe	16	-160	6350	6250	17.3	17.2	+ 1.0	6350	6250	609	2135
8	Probe	15	-150	7750	7650	17.5	16.3	+12.0	7750	7650	655	2200
9	Probe	23	-230	7550	7450	19.9	16.7	+32.0	7550	7450	664	2204

through this wedge until it had gone about 1000 nautical miles from Nandi. A cold front was crossed at about 1300 nautical miles, and the flight then continued on to Sydney in a maritime polar air mass.

The cloud diagram (Fig. 10) and the weather map (Fig. 11) show a cold front at about 1300 nautical miles from Nandi. The soundings for Norfolk Island, Lord Howe Island, and Williamtown (Fig. 10) show similar characteristics but are quite different from that for Nandi (Fig. 10). The 23Z, February 12, 1962, Nandi sounding shows potential temperatures from 315 to 303 degrees Kelvin, and moistures from 8 to 18 grams per kilogram, but the Norfolk Island, Lord Howe Island, and Williamtown soundings show potential temperatures from 303 to 296 degrees Kelvin, and specific humidities from 1.3 to 12.6 grams per kilogram. This drop in temperature and moisture is indicative of a change in air mass, namely from maritime tropical to maritime polar. The Norfolk Island sounding is similar to Lord Howe Island and Williamtown soundings because the cold front passed the station before the sounding was taken, thus changing the air mass from maritime tropical to maritime polar. Neither the aircraft sounding at Sydney nor the radiosonde observation showed radio duct formation in this region at the flight level, but the Lord Howe Island sounding showed a strong radio duct formation at 9.1 to 8.8 thousand feet (722 to 730 mb). The Williamtown sounding does not go high enough to verify the extent of this layer.

Table 6  
Refractive Index Gradients,  
Nandi, Fiji, 23Z,  
February 10, 1962

Layer (10 <sup>3</sup> ft)	dN/dh
9.9 to 6.5	- 8
6.5 to 4.8	- 8
4.8 to 0.2	-10

The radio duct conditions for this flight are considered to be from 450 to 950 nautical miles from Nandi in the subsidence region of the high pressure wedge. Notice that there are three layers present in this wedge (Fig. 10). The cloud diagram shows that the radio duct layer at point 1 of Table 7 (and Fig. 10) is of very limited extent.

Considering the 1775 nautical miles flown on this mission, approximately 475, or about one-fourth showed refractive index gradients favorable for radio duct formation.

#### Mission 5, Sydney, Australia, to Perth, Australia

Propagation effects at vhf were observed along the central southern coast of Australia from Sydney to Perth. The warm dry continental air blown off the land formed a steep moisture gradient when it overlaid the cool moist maritime air masses along the path.

The maritime polar air mass of potential temperature ranging from 297 to 303 degrees Kelvin and moisture of 12.5 to 5.2 grams per kilogram shown by the Williamtown

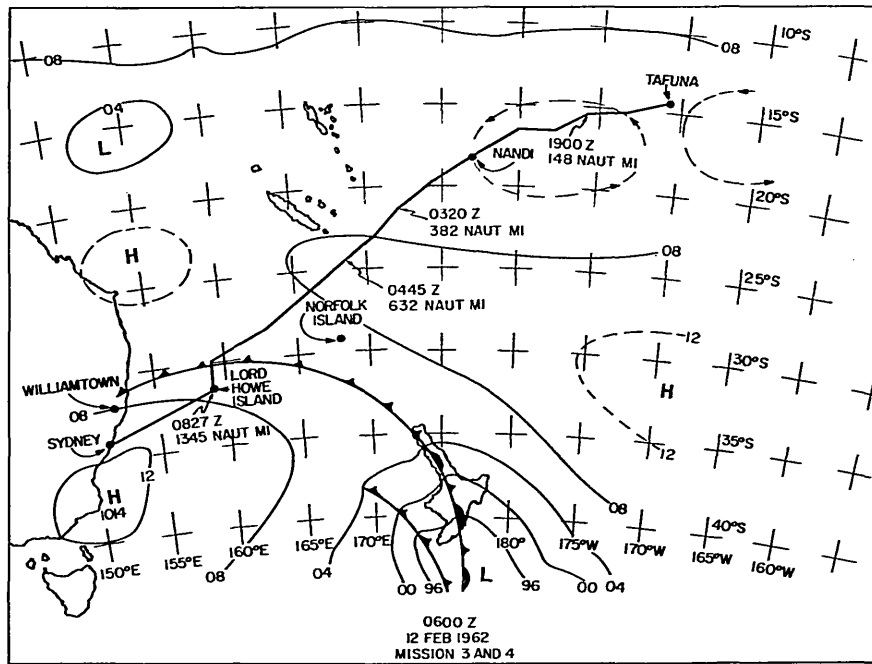


Fig. 11 - Sea-level pressure chart for the area between Tafuna, Samoa, to Sydney, Australia (Missions 3 and 4)

Table 7  
Summary of Mission 4

Position Number	Sounding or Probe	N-break (N-units)	dN / 1000 ft	Layer		Temperature		dT / 1000 ft	Layer		Distance (naut mi)	Time (Z)
				Top (ft)	Base (ft)	Top (°C)	Base (°C)		Top (ft)	Base (ft)		
1	Probe	15	-150	6000	5900	16.6	17.5	- 9.0	6000	5900	45	0128
2	Probe	15	-150	5500	5400	15.3	15.2	+ 1.0	5500	5400	708	0511
3	Probe	17	-170	5400	5300	16.5	16.4	+ 1.0	5400	5300	718	0518
4	Probe	31	-310	5350	5250	17.6	16.5	+11.0	5350	5250	738	0521
5	Probe	20	-200	5400	5300	17.0	16.6	+ 4.0	5400	5300	750	0525
6	Sounding	30	- 86	6750	6400	13.9	13.6	+ 1.0	6750	6400	811	0545
7	Sounding	20	-133	6900	6750	14.4	13.9	+ 0.7	6900	6750	868	0602
8	Sounding	20	- 67	1850	1550	21.0	21.7	- 2.3	1850	1550	868	0604

Table 8  
Refractive Index Gradients

Nandi, Fiji, 23Z, February 12, 1962		Norfolk Island, 23Z, February 12, 1962		Lord Howe Island, 23Z, February 12, 1962		Williamtown, 23Z, February 12, 1962	
Layer (10 <sup>3</sup> ft)	dN/dh	Layer (10 <sup>3</sup> ft)	dN/dh	Layer (10 <sup>3</sup> ft)	dN/dh	Layer (10 <sup>3</sup> ft)	dN/dh
10.0 to 7.05	-11	4.8 to 3.5	-22	9.1 to 8.8	-40	8.8 to 4.45	- 5
7.05 to 5.1	-20	3.5 to 0.9	-12	8.8 to 5.4	-12	4.45 to 0.75	-12
5.1 to 2.9	-10			5.4 to 4.8	- 6		
2.9 to 0.6	-17			4.8 to 0.95	- 6		

radiosonde observation (Fig. 10) for 23Z, February 12, 1962, is considerably moister and warmer than the maritime polar air mass shown by the Adelaide, Australia, radiosonde observation, 00Z February 13, 1962 (Fig. 12), which has a potential temperature range of 289 to 297 degrees Kelvin and a moisture range of 6 to 1.4 grams per kilogram. This is because two occluded fronts separated the air masses over Sydney and Adelaide. The northerly flow of maritime polar air experienced at Williamstown had acquired heat and moisture from its trajectory over warmer water and land and was therefore warmer than the air mass experienced behind the occluded fronts, where the air had a trajectory over colder water as shown by the Adelaide characteristic curve. The circulation of the anticyclone centered at 36°S and 130°E (Fig. 13) brought maritime polar air over the dry land in a southerly current of air which had passed over a relatively colder water surface.

The first occluded front was noticeable by rain falling from very high clouds. The rain did not appear to reach the ground. The second occluded front was not very pronounced.

A haze layer was observed when the aircraft was near Adelaide, Australia, and continued for 800 nautical miles. Another haze layer was present at about 8000 feet, but it was hard to judge the continuity of the upper layer. The moisture carried in by the southerly winds from the ocean was trapped under an upper layer of dry subsiding air. This stratification caused by subsidence in the anticyclone is shown on the Adelaide and Forrest soundings (Fig. 12). The layer was much shallower at Adelaide, being from 4300 to 4200 feet, than it was at Forrest, being from 4800 to 3600 feet (Table 9). This layer is in agreement with the haze layer as observed on the cloud chart (Fig. 12). The top of the haze layer is the potential temperature surface at 295-296 degrees Kelvin for both locations.

The approach to the low-pressure trough of the weather map is clearly shown on the Kalgoorlie 23Z, February 13, 1962, radio sounding (Fig. 12); the moisture curve shows warm moist maritime tropical air overrunning the maritime polar air which has a maximum of 13.5 grams per kilogram at 4800 feet. No ducts are indicated by the radiosonde observation for this station. The cloud bases were at an altitude of 6000 feet, and the rainfall did not appear to reach the ground (Fig. 12).

At Guildford, Australia, near Perth (Fig. 12) the radiosonde curve for 23Z, February 13, 1962, shows maritime polar air in the lower layers with remnants of the maritime tropical air from the trough shown above 6400 feet (800 mb) as indicated by the increase in moisture above this level. No duct formation is observed on the radiosonde refractive index curve.

The estimated extent of the radio duct on this mission is coincident with that of the haze layer observed from 600 nautical miles to 1400 nautical miles from Sydney. The presence of a radio duct at about 2200 feet at 950 nautical miles from Sydney was confirmed by the reception of the radio range signals from Ceduna at 109.9 Mc. Points 2 and 3 in Fig. 12 show the distances and altitudes where the signals were heard. The radio range station was also heard in this location at 7500 feet, but duct formation is doubted at this altitude because the radio horizon was only 30 nautical miles away. At point 3 the radio horizon was 67 nautical miles and the aircraft was over 100 nautical miles from Ceduna (32.1° S, 133.8° E). A radio duct is necessary for reception at this height and distance.

Points 2 and 3 in Table 9 (and Fig. 12) show refractive index gradients of -78 and -71 N-units/1000 feet, respectively, and temperature inversions of +4.2 and +3.1°C/1000 feet, respectively. This gives additional confirmation to the vhf radio signal duct formation at the lower haze layer. Points 1 and 4 of Table 9 were for discontinuous layers and were not considered to represent a radio duct.

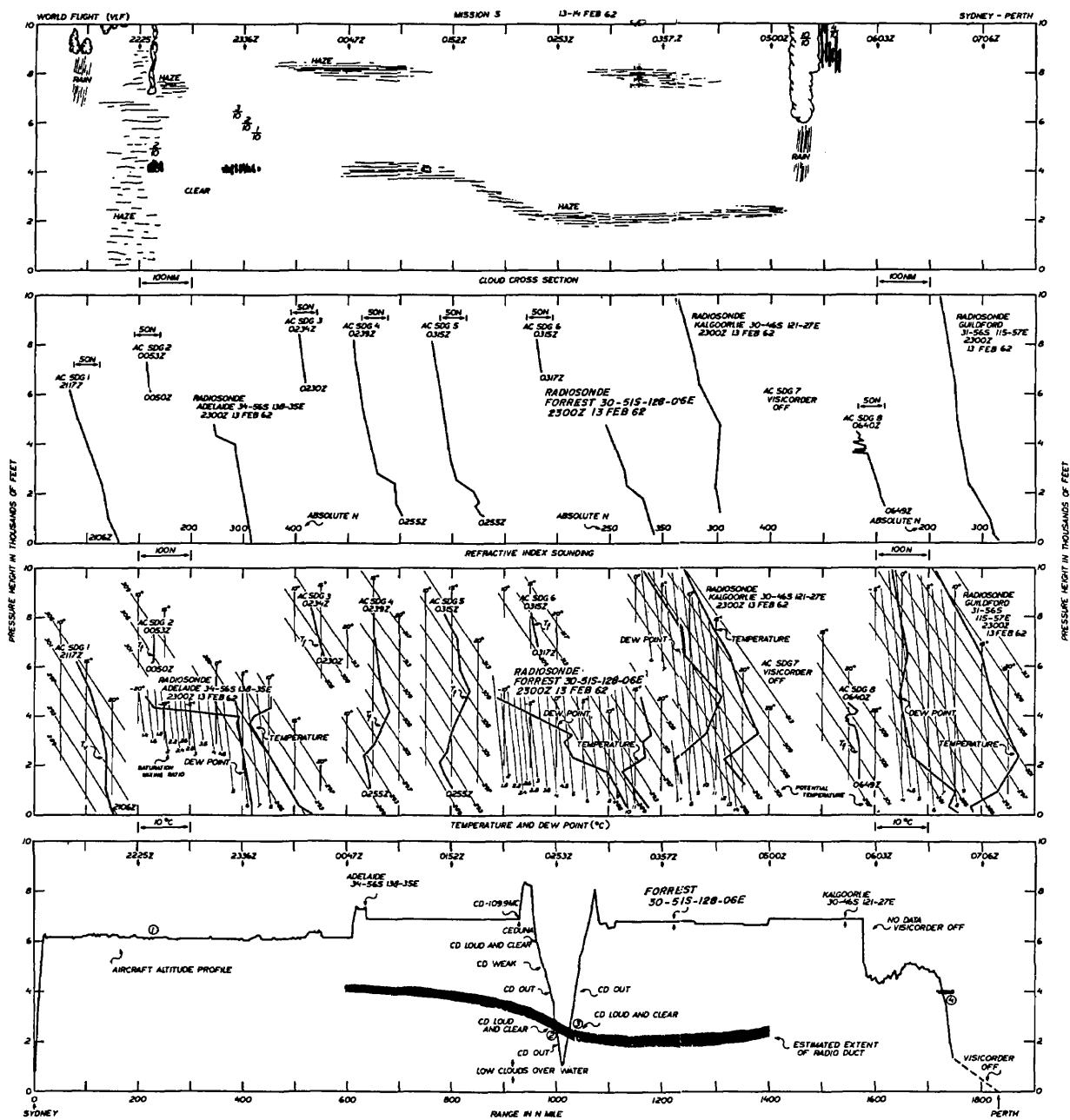


Fig. 12 - Cross section of meteorological conditions from Sydney, Australia, to Perth, Australia (Mission 5)

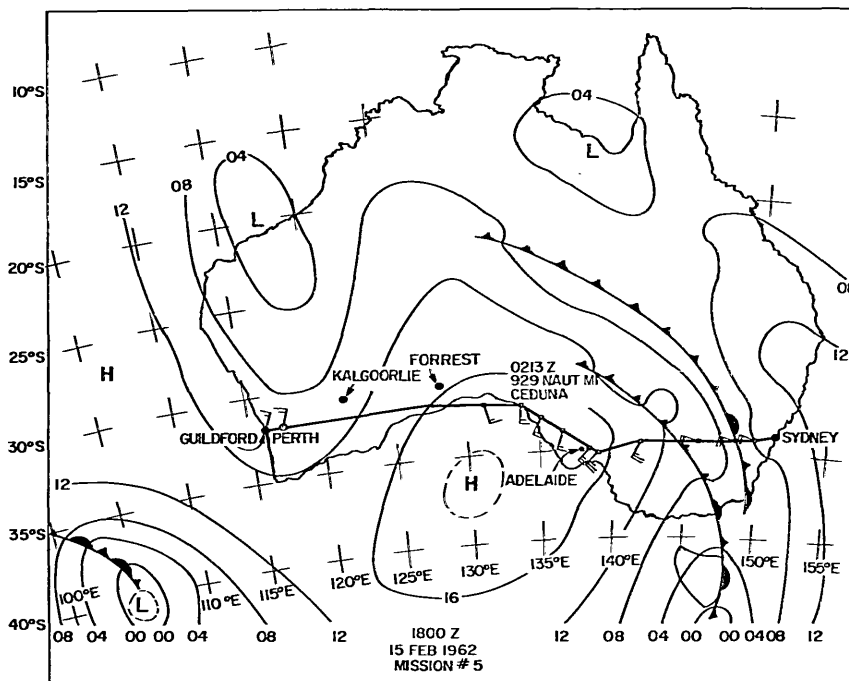


Fig. 13 - Sea-level pressure chart for the area between Sydney, Australia, to Perth, Australia (Mission 5)

Table 9  
Summary of Mission 5

Position Number	Sounding or Probe	N-break (N-units)	dN / 1000 ft	Layer		Temperature		dT / 1000 ft	Layer		Distance (naut mi)	Time (Z)
				Top (ft)	Base (ft)	Top (°C)	Base (°C)		Top (ft)	Base (ft)		
1	Probe	34	-340	6200	6100	14.1	13.5	+6.0	6200	6100	229	2235
2	Sounding	35	- 78	2850	2400	15.2	13.3	+4.2	2850	2400	1003	0254
3	Sounding	32	- 71	2550	2100	14.2	12.8	+3.1	2550	2100	1022	0300
4	Sounding	20	-133	4050	3900	20.0	19.5	+3.3	4050	3900	1733	0645

Table 10  
Refractive Index Gradients

Adelaide, Australia, 23Z, February 13, 1962		Forrest, Australia, 23Z, February 13, 1962		Kalgoorlie, Australia, 23Z, February 13, 1962		Guildford, Australia, 23Z, February 13, 1962	
Layer (10 <sup>3</sup> ft)	dN/dh	Layer (10 <sup>3</sup> ft)	dN/dh	Layer (10 <sup>3</sup> ft)	dN/dh	Layer (10 <sup>3</sup> ft)	dN/dh
4.8 to 4.3	-10	4.8 to 3.2	-30	9.9 to 7.6	-12	9.9 to 6.4	- 5
4.3 to 4.0	-75	3.2 to 3.0	-30	7.6 to 6.4	-10	6.4 to 4.8	- 1
4.0 to 0.4	-12	3.0 to 2.3	-15	6.4 to 4.8	-22	4.8 to 2.3	- 5
		2.3 to 1.8	-55	4.8 to 3.2	- 4	2.3 to 0.9	-29
		1.8 to 0.4	-15	3.2 to 2.2	+ 1	0.9 to 0.4	-23
				2.2 to 1.2	-10	0.4 to 0.1	-60

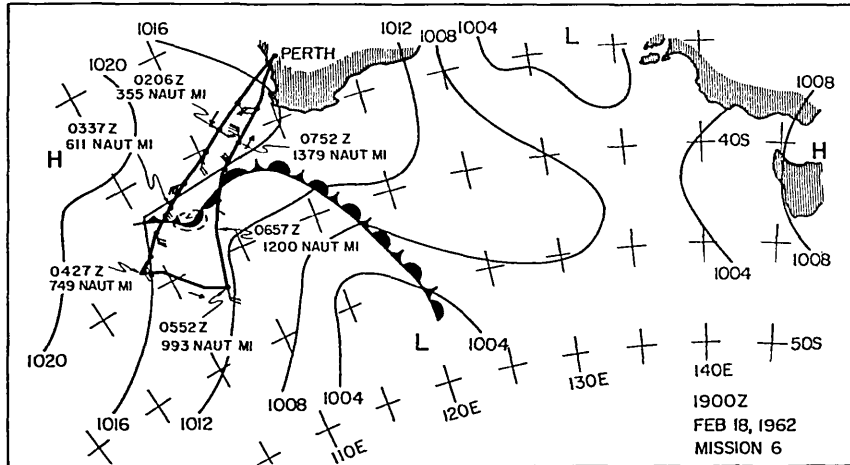


Fig. 14 - Sea-level pressure chart for the area covered in the first flight from Perth, Australia (Mission 6)

Considering that only about 300 nautical miles of this mission were flown over water, duct formation of vhf and uhf radio signals occurred 100% of the time. Figure 12 shows that the estimated extent of the duct was 800 nautical miles; hence 500 nautical miles of this duct formation occurred over land.

#### Mission 6, Perth, Australia, Local Flight 1

The Mission 6 flight, all over water (Fig. 14), crossed a narrow high-pressure wedge, a frontal system at 37°S, 105°E, proceeded again in a high-pressure circulation from 39°S, 104°E to 42°S, 108°E, and then returned to Perth, crossing the frontal system again at 37°S, 110°E.

The radiosonde observation for Guildford (Fig. 17) for 23Z on the following day, February 19, 1962, shows the air mass to be maritime polar because the potential temperature values of 289 to 306 degrees Kelvin and specific humidities of 8 to 2.4 grams per kilogram are typical for the altitude range from the surface to 10,000 feet.

The weather map (Fig. 14) shows that the air mass south of the frontal system was also of maritime polar origin, and the frontal discontinuity indicates that the northward flowing air is being modified as it progresses from colder to warmer water. A weak convergence is taking place at the frontal zone.

Table 11 shows that refractive index gradients capable of supporting radio duct formation were measured at points 1, 2, 3, 5, 6, 7, 8, 9, and 10 (Fig. 15). However these points are not all in a continuous layer, as seen on the cloud diagram and the duct diagram.

Points 1, 2, and 3 were measured in the high-pressure wedge, where anticyclonic flow was shown by the isobars. The negative refractive index gradients show a radio duct formation. The positive temperature gradients show subsidence. These points were in a continuous layer. The trend toward subsidence in this wedge is being broken up by the approach of the frontal system at about 650 nautical miles from Perth.

Points 5, 6, and 7, measured after crossing the cold front, show radio duct formation conditions with negative refractive index gradients and subsidence with (stable) temperature gradients of +3.7°C/1000 feet, +4.6°C/1000 feet, and +17.0°C/1000 feet, respectively.

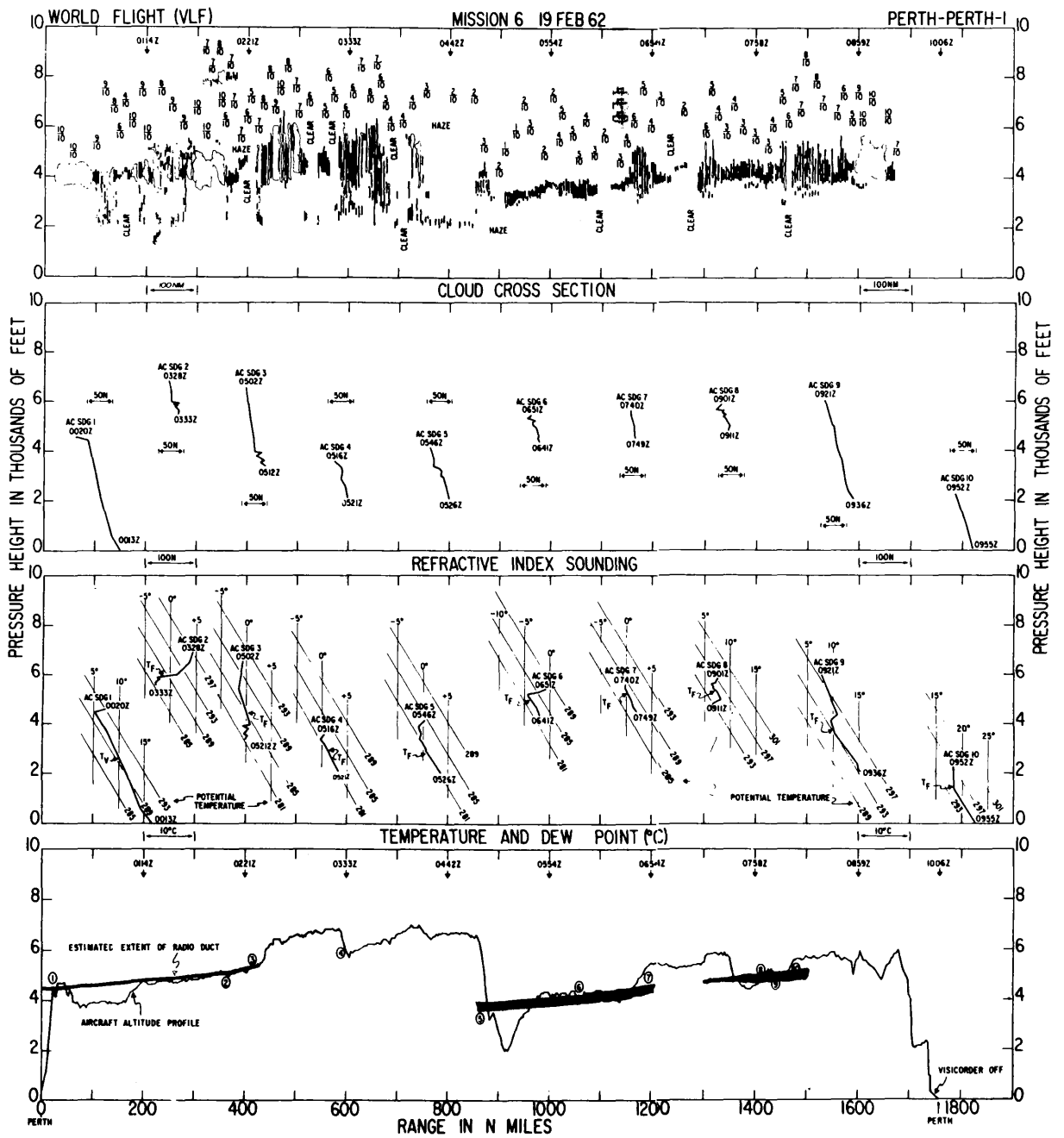


Fig. 15 - Cross section of meteorological conditions in the first flight from Perth, Australia (Mission 6)

Table 11  
Summary of Mission 6

Position Number	Sounding or Probe	N-break (N-units)	dN 1000 ft	Layer		Temperature		dT 1000 ft	Layer		Distance (naut mi)	Time (Z)
				Top (ft)	Base (ft)	Top (°C)	Base (°C)		Top (ft)	Base (ft)		
1	Sounding	24	-240	4550	4450	+10.5	+5.4	+51.0	4500	4400	12	0015
2	Probe	25	-250	5150	5050	+ 7.5	+6.8	+ 7.0	5150	5050	361	0208
3	Probe	22	-220	5400	5300	+ 5.5	+0.5	+50.0	5400	5300	415	0220
4	Sounding	16	---	6000	5950	+ 1.1	-0.8	--	6000	5950	596	0330
5	Sounding	19	- 54	3950	3600	+ 0.8	-0.5	+ 3.7	3950	3600	870	0507
6	Probe	19	- 54	4200	3850	- 0.7	-2.3	+ 4.6	4200	3850	1061	0613
7	Sounding	15	-150	5300	5200	- 0.9	-4.3	+17.0	5400	5200	1174	0646
8	Sounding	23	-230	4900	4800	+ 0.4	-0.6	+10.0	4900	4800	1416	0804
9	Probe	19	-190	5100	5000	+ 1.3	+3.6	-23.0	5100	5000	1435	0810
10	Sounding	22	-147	5500	5350	+ 2.4	-0.5	+12.6	5500	5350	1467	0822
11	Sounding	15	---	5650	5600	+ 7.0	+6.1	--	5650	5600	1624	0906

Table 12  
Refractive Index Gradients  
Guildford, Australia, 23Z,  
February 19, 1962

Layer (10 <sup>3</sup> ft)	dN/dh
9.9 to 7.4	- 7
7.4 to 4.8	-10
4.8 to 0.4	- 7

These positive temperature gradients would indicate that air was subsiding and that the duct layer should strengthen. This indication is in agreement with Eq. (7), which states that for southerly flow (in the Southern Hemisphere) the vorticity should be decreasing (increasing divergence or subsidence by Eq. (2)).

Points 8, 9, and 10, measured after crossing the front on the return portion of the mission, indicate radio duct formation conditions again. Points 8 and 10 indicate positive temperature gradients of +10.0°C/1000 feet and +12.6°C/1000 feet, respectively, which is indicative of subsidence by Eqs. (2) and (9). Point 9 shows a gradient of -23.0°C/1000 feet. This could indicate a change from subsiding air to rising air at this point and would indicate the advance of the approaching front and the breaking up of the layer.

Refractive index gradients, cloud structure, and temperature gradients indicate radio duct formation over almost one-third the total flight distance of 1750 nautical miles.

Mission 7, Perth, Australia, Local Flight 2

The plan for the second local flight out of Perth was a triangular pattern similar to that for the previous day except that the direction of the flight was in a clockwise direction (Fig. 16). The pressure gradients in the anticyclone and the frontal zone were weaker.

The cloud structure shown in the cross section (Fig. 17) indicates stratification (subsidence) over most of the route except for the frontal zones. However the aircraft

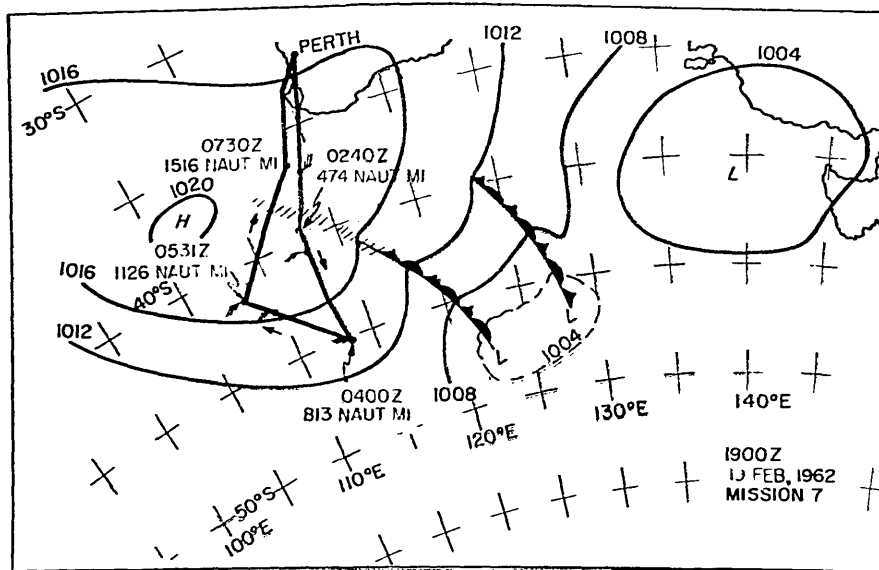


Fig. 16 - Sea-level pressure chart for the area covered in the second flight from Perth, Australia (Mission 7)

soundings at 2356Z and 0037Z and the Guildford radiosonde observation 23Z, February 19, 1962, do not show radio duct formation. For a 100-nautical-mile stretch beginning at 0050Z there was a continuous cloud layer which appeared to be a duct, but outside of that the clouds were thin and scattered and of not sufficient continuity. Subsidence in itself is not sufficient to cause anomalous propagation. There must be at least enough moisture present to create the refractive index gradient of  $-48.6$  N-units/1000 feet required for bending tangentially propagated radio waves with a curvature equal to that of the earth (7).

After the flight crossed the weak front at 0147Z, continuous cloud layers were found. The aircraft sounding at 0600Z, point 1 in Table 13 (and Fig. 17), shows a gradient of  $-48$  N-units/1000 feet (barely enough to support a duct) and a temperature gradient of  $+12.5^{\circ}\text{C}/1000$  feet, but at the 0620Z sounding the refractive index gradient was not strong enough to support a radio duct. The 0620Z position was made in the frontal zone, and the temperature gradient had lessened to  $+4.6^{\circ}\text{C}/1000$  feet, which shows decreasing subsidence or increasing convergence. Beginning at 0720Z the cloud structure again appeared to support radio duct formation. Points 2 and 3 in Table 13 show refractive index gradients of  $-70$  N-units/1000 feet with positive temperature gradients of  $+18.3^{\circ}\text{C}/1000$  feet and  $+14.3^{\circ}\text{C}/1000$  feet, respectively.

It is estimated that radio ducts were present for more than one-half of the 1825 nautical miles flown on this mission. The weather map and the temperature inversions in the soundings would suggest that more radio ducts should be present, but the lack of moisture in the lower layers prevented more extensive layers.

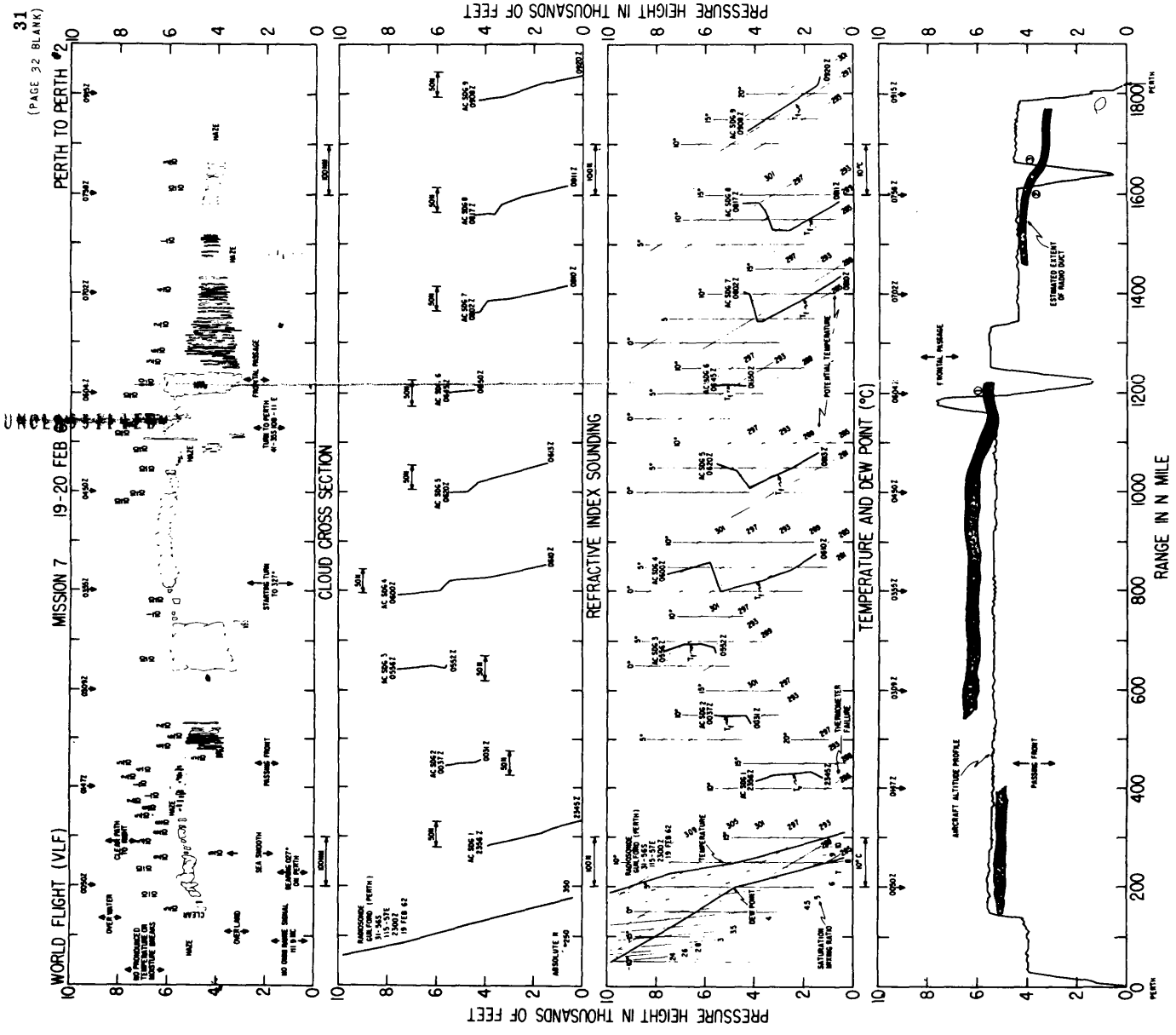


Fig. 17 - Cross section of meteorological conditions in the second flight from Perth, Australia (Mission 7)

Table 13  
Summary of Mission 7

Position Number	Sounding or Probe	N-break (N-units)	dN/1000 ft	Layer		Temperature		dT/1000 ft	Layer		Distance (naut mi)	Time (Z)
				Top (ft)	Base (ft)	Top (°C)	Base (°C)		Top (ft)	Base (ft)		
1	Sounding	19	-48	5800	5400	+ 5.8	+0.8	+12.5	5800	5400	1200	0606
2	Sounding	21	-70	4200	3900	+10.0	+4.5	+18.3	4200	3900	1626	0806
3	Sounding	21	-70	3600	3300	+12.3	+8.0	+14.3	3600	3300	1652	0814

Table 14  
Refractive Index Gradients,  
Guildford, Australia, 23Z,  
February 19, 1962

Layer (10 <sup>3</sup> ft)	dN/dh
9.9 to 7.4	- 7
7.4 to 4.8	-10
4.8 to 0.4	- 7

#### Mission 8, Perth, Australia, Local Flight 3

The third local flight out of Perth progressed southward from Perth to a point at 45°S, 113°E, then northward to 35°S, 120°E, and then overland to Perth. The southern portion of the flight was in a warm front zone, but the rest of the flight was in maritime polar air (Fig. 18). The radiosonde observation for Guildford, 23Z, February 20, 1962, shows conservative air mass properties of potential temperature and specific humidity typical of maritime polar air above 1600 feet (Fig. 19), but below this level the specific humidity becomes very dry. This dryness is the effect of air having a long trajectory over dry land.

The radiosonde observation for Guildford shows no indication of radio duct formation. This is because the air reaching Guildford was approaching from the east and had a trajectory over land. However, not all of the air parcels measured in the flight had their trajectory over land, and the lower layers were more moist. This is shown by the cloud layer (Fig. 19) from 300 to 650 nautical miles from Perth (0130Z to 0300Z). The measured refractive index gradients from points 1, 2, 3, 5, 7, 8, and 9 show strong refractive index gradients (Table 15 and Fig. 19) and the temperature gradients at these points are positive, showing a strong temperature inversion which is suggestive of subsidence (Eq. (9)).

In contrast to the area of subsidence or divergence, the frontal zone was an area of convergence. The rain encountered in this area is an indication of rising currents of air, which are not favorable for the formation of duct layers. No refractive index gradients capable of supporting radio duct formation (less than -48.6 N-units/1000 feet) were measured from 650 to 1150 nautical miles from Perth (0330 to 0500Z).

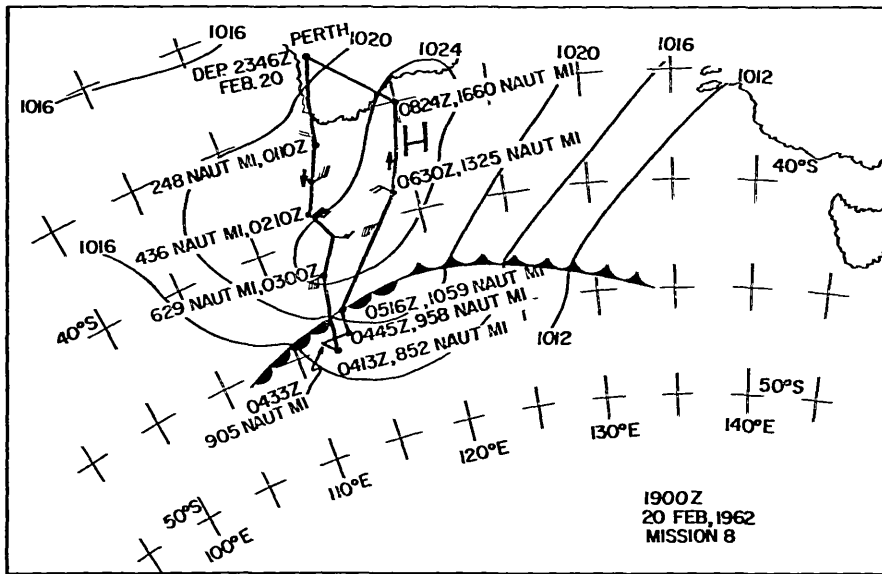


Fig. 18 - Sea-level pressure chart for the area covered in the third flight from Perth, Australia (Mission 8)

From 1200 to 1550 nautical miles the flight was in the same air mass as the south-bound trip (0600 to 0745Z). Again points 10, 11, 12, 13, 14, and 15 (Table 15 and Fig. 19) show strong refractive index gradients and positive temperature gradients, which are indicative of a pronounced radio duct layer.

At about 1600 nautical miles from Perth (0800Z) the cloud layer disappeared and the duct layer vanished. The moist air from the ocean was now being replaced by the dry air from off the continent.

It is estimated that 700 of the 1900 nautical miles flown on this mission were in conditions favorable for radio ducts, or more than one-third of the flight mileage.

This flight is an excellent example of the principles shown by vorticity theory; namely, (a) radio duct formation is affected by the trajectory of the air mass parcels, since subsidence must take place over moist air; (b) regions of divergence (anticyclones) are favorable for radio duct formation; and (c) regions of convergence (fronts) are not favorable for radio duct formation.

#### Mission 9, Perth, Australia, to Singapore

The flight from Perth to Singapore was along the western coast of Australia and across the Indian Ocean to the Malayan Peninsula (Fig. 20).

The weather map indicated that the same anticyclonic circulation was present in southwest Australia as was there on the previous mission. It would be expected that the winds blowing off the continent transported maritime polar air that was dry in the lower layers, as was shown in the Guildford radiosonde observation (Fig. 19) for February 20, 1962. This condition was characterized by clear skies for about the first 600 nautical miles of the flight, until the path left the shoreline and started crossing the Indian Ocean at 0400Z.

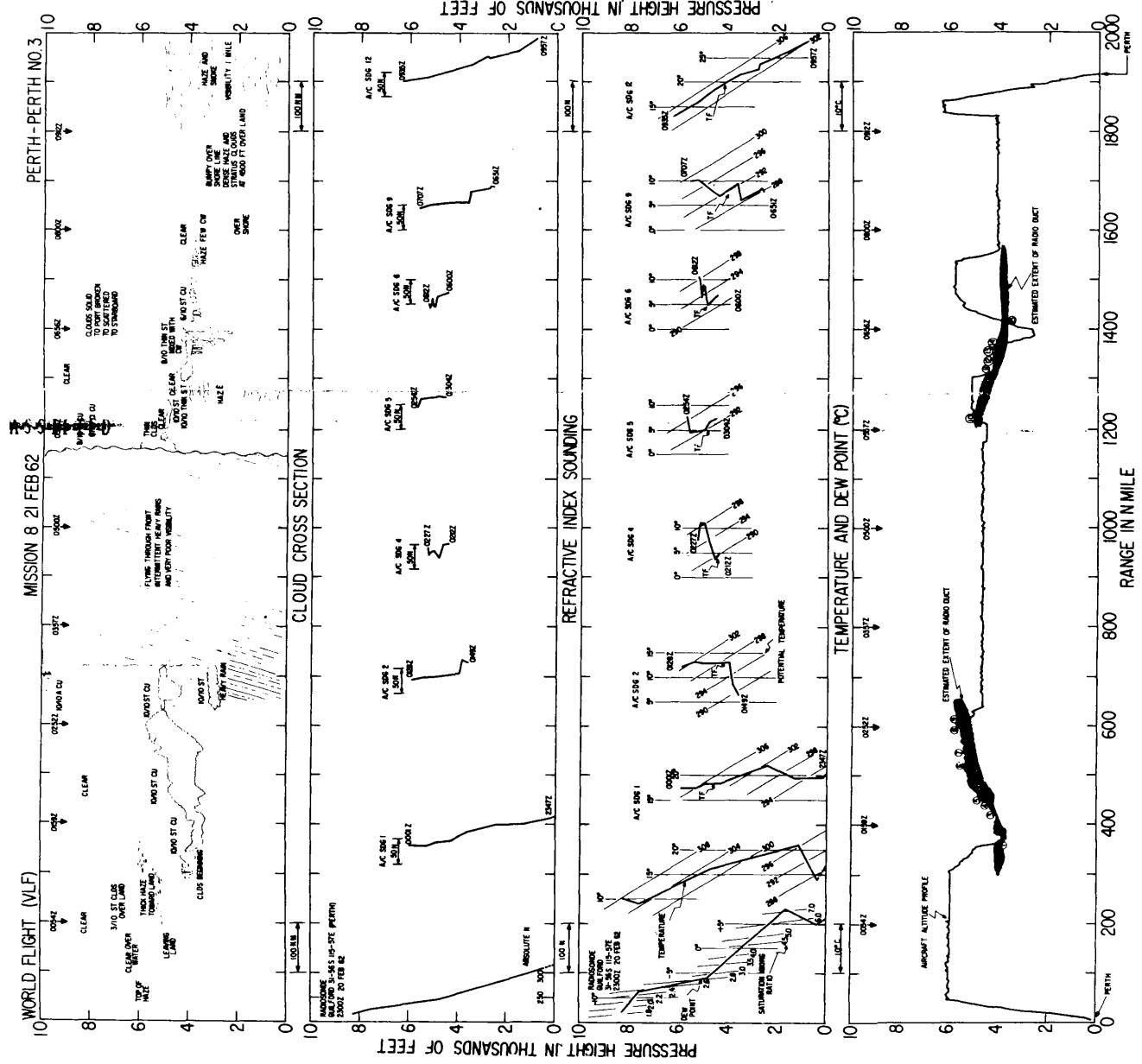


Fig. 19 - Cross section of meteorological conditions in the third flight from Perth, Australia (Mission 8)



After crossing a slight high pressure wedge over the Indian Ocean a weak disturbance was encountered at  $16^{\circ}\text{S}$ ,  $111^{\circ}\text{E}$ . In this area the upper clouds appeared to be circular bands. In progressing northward from this weak disturbance there was slight turbulence in the clear air. Upon approaching the Malayan Peninsula the clouds built up to heights over 10,000 feet. Along the peninsula the path was alternately over land and water. Over land there were towering cumulus clouds.

The Singapore 00Z, February 22, 1962, radiosonde (Fig. 21) shows values of potential temperature and specific humidity which are typical of maritime air masses. Neither the radiosonde observation nor the refractometer measurements made in flight indicated large refractive index breaks. Position 1 in Table 17 (and Fig. 21) shows a short radio duct layer, about 40 nautical miles, but this was not extensive enough to be considered a layer.

It is interesting to compare this flight, Mission 9, with the last 450 nautical miles of Mission 2, and all of Mission 3. In Missions 2 and 3 the flight was either in modified maritime polar or maritime tropical air mass, and there was a strong convergence zone. Towering cumulonimbus clouds were present, and there was an abundance of rain. Continuous radio duct layers were not present in this region south of the equator. Mission 9 also shows a convergence zone between  $5^{\circ}$  and  $10^{\circ}\text{S}$ . With the presence of convergence and cyclonically curved isobars Eqs. (2) and (3) would suggest that if there were any subsidence, it would be decreasing with time, and that radio duct formation would not be expected. The observations made during the flight substantiate this conclusion. However, it is quite possible that radio duct conditions were present off the western coast of Australia, but this was not along our line of flight.

#### Mission 10, Singapore to Bangkok, Thailand

The same maritime tropical air mass as was present at Singapore, on February 22, continues to be present at both Singapore and Bangkok. The potential temperature and specific humidity values show a typical maritime tropical air mass at both locations for the February 24, 00Z radiosonde observations (Fig. 22). The soundings do not show any refractive index layers suitable for radio duct formation.

The weather map (Fig. 23) shows very weak gradients over the flight path. Since the gradients are so weak, it suggests that little if any convergence is present, except for a very weak orographic low at  $10^{\circ}\text{N}$ ,  $102^{\circ}\text{E}$ . This conclusion is supported by the cloud diagram (Fig. 22), which shows stratified type clouds except for towering cumulus clouds over the shoreline. In this vicinity, 200 to 300 nautical miles north of Singapore and just before reaching Bangkok, cumulus buildups were observed.

Positions 1, 2, and 3 of Table 19 (and Fig. 22) show refractive index gradients which support radio duct formation, i.e., less than  $-48.6$  N-units/1000 feet. The temperature gradients for these points also support the conclusion that subsidence is taking place, because points 2 and 3 show  $+6.4$  and  $+3.0^{\circ}\text{C}/1000$  feet. Position 4 in Table 19 shows a refractive index gradient which supports a duct, but the temperature gradient is  $-15^{\circ}\text{C}/1000$  feet, which indicates that there is a tendency toward convergence in this region as is suggested by the orographic low on the weather map.

Aircraft soundings 1, 2, 3, and 4 (Fig. 22) show positive refractive index gradients. If the refractive index gradient is greater than  $-12.6$  N-units/1000 feet, it is known as substandard propagation (7). This means that the radio range will be less than the line-of-sight horizon for standard propagation. Sounding 1 shows tops of such a layer at 2500 feet and 3800 feet, sounding 2 at 3500 feet, sounding 3 at 3700 and 5000 feet, and sounding 4 at 7500 feet. The radio sounding at Bangkok shows such a layer at the surface.

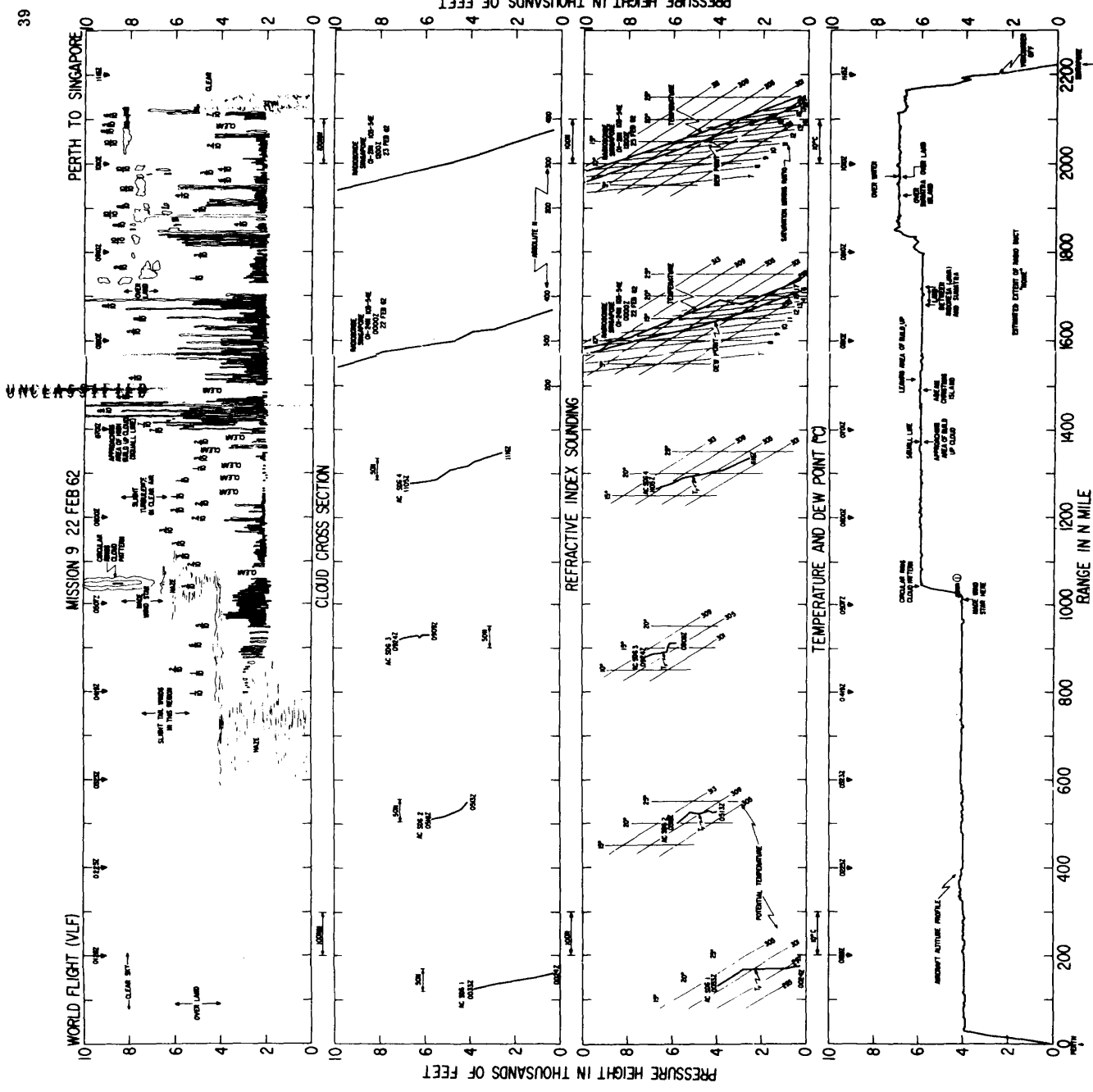


Fig. 21 - Cross section of meteorological conditions in the flight from Perth, Australia, to Singapore (Mission 9)



Table 17  
Summary of Mission 9

Position Number	Sounding or Probe	N-break (N-units)	dN / 1000 ft	Layer		Temperature		dT / 1000 ft	Layer		Distance (naut mi)	Time (Z)
				Top (ft)	Base (ft)	Top (°C)	Base (°C)		Top (ft)	Base (ft)		
1	Sounding	16	-80	4350	4150	22.7	22.4	+1.5	4350	4150	1035	0516

Table 18  
Refractive Index Gradients,  
Singapore, 00Z,  
February 22, 1962

Layer (10 <sup>3</sup> ft)	dN/dh
9.9 to 7.9	-10
7.9 to 4.8	- 8
4.8 to 3.9	-30
3.9 to 2.95	-10
2.95 to 0.35	- 8
0.35 to 0.0	-20

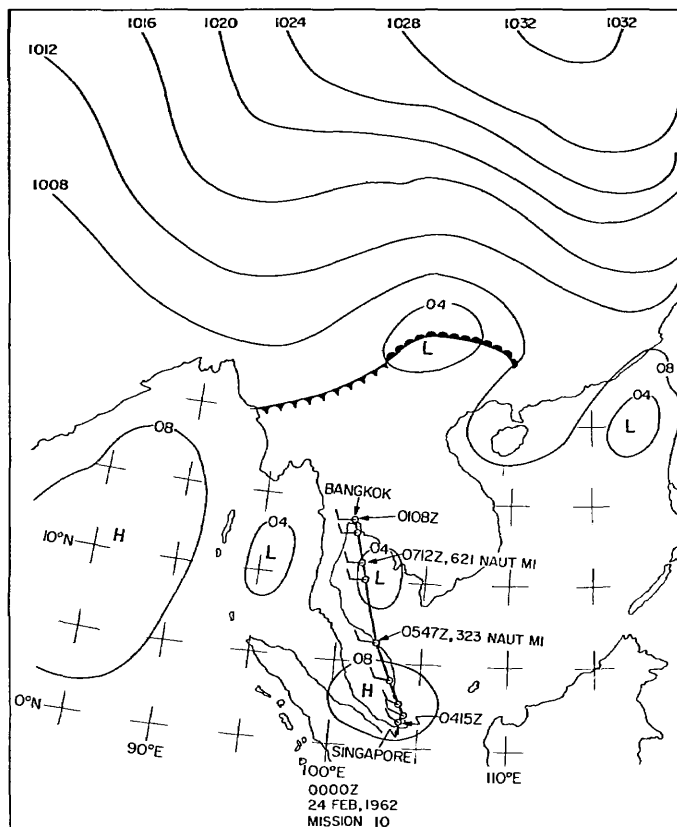


Fig. 23 - Sea-level pressure chart for the area covered in the flight from Singapore to Bangkok, Thailand (Mission 10)

Table 19  
Summary of Mission 10

Position Number	Sounding or Probe	N-break (N-units)	dN 1000 ft	Layer		Temperature		dT 1000 ft	Layer		Distance (naut mi)	Time (Z)
				Top (ft)	Base (ft)	Top (°C)	Base (°C)		Top (ft)	Base (ft)		
1	Sounding	18	- 60	3400	3100	--	--	--	--	--	39	0422
2	Sounding	38	-152	2750	2500	+21.0	+19.4	+ 6.4	2750	2500	383	0604
3	Sounding	37	-123	3000	2700	+20.0	+19.1	+ 3.0	3000	2700	454	0624
4	Probe	31	-310	3400	3300	+19.7	+21.2	-15.0	3400	3300	778	0759

Table 20  
Refractive Index Gradients

Singapore, 00Z, February 24, 1962		Bangkok, Thailand, 00Z, February 24, 1962	
Layer (10 <sup>3</sup> ft)	dN/dh	Layer (10 <sup>3</sup> ft)	dN/dh
9.90 to 4.80	-10	9.90 to 4.80	-12
4.80 to 0.35	-14	4.80 to 0.35	-10
		0.35 to 0.10	+20

Again it is interesting to compare this flight with the portion of Mission 2 which was north of the equator. Except for the distorting effect of the land the two missions compare very favorably. In both missions radio duct conditions were present, about four-fifths of the distance on Mission 2, and about one-half of the 800-nautical-mile distance on Mission 10. These results seem to support the conclusion that the tropics can be a region of radio duct formation at vhf, if there is subsidence, or divergence, indicated by the clouds formation, the weather map, and the soundings.

#### Mission 11, Bangkok, Thailand, to Calcutta, India

Both Bangkok and Calcutta are in a maritime tropical air mass. As was the case in Mission 10 the weather map (Fig. 24) shows a very flat pressure field. The first 600 nautical miles of the flight going westward from Bangkok over the Bay of Bengal was through a very weak trough. From the 600-nautical-mile point (0423Z) the flight continued in a very weak ridge of high pressure to 15°N, 85°30'E. The direction of the flight then changed to the north, and as it approached land another trough was entered.

Although there was considerable haze, as shown by the cloud diagram, duct formation was not measured until the aircraft entered a cloud layer. Points 2, 3, 4, and 5 of the flight profile (Fig. 25) and points 2, 3, 4, and 5 of Table 21 show refractive index gradients and positive temperature gradients favorable for radio duct formation. The positive temperature gradients indicate that subsidence has taken place. The clouds in this region are of the convective type, but when the convective currents encounter the strong positive temperature gradients, moisture spreads out in a moist/dry interface which is favorable for radio duct formation.

Position 1 in Table 21 shows a duct layer, but this was measured over land and there were no convective cloud chimneys to maintain a layer of moisture against the isothermal temperature gradient layer.

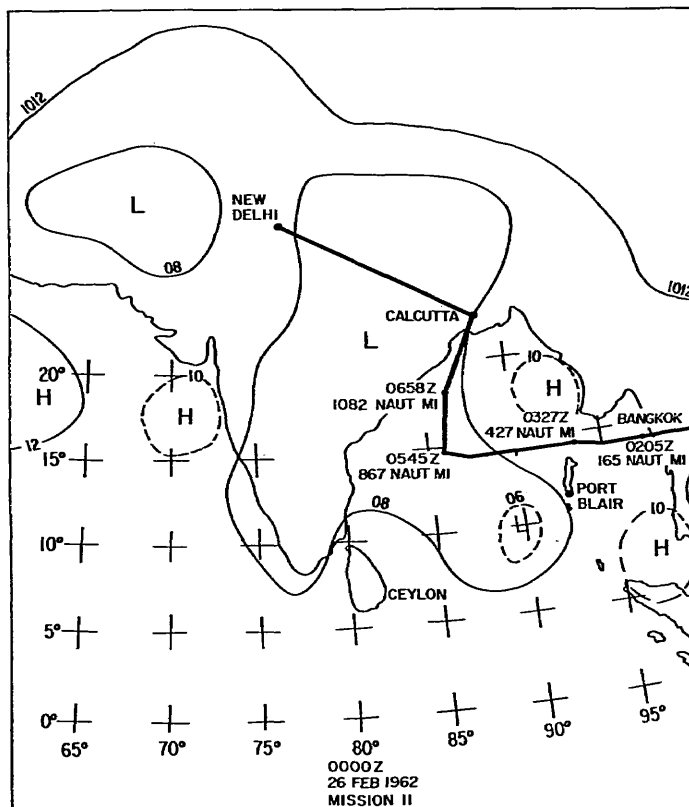


Fig. 24 - Sea-level pressure chart for the area covered in the flight from Bangkok, Thailand, to Calcutta, India (Mission 11)

As shown by the flight profile (Fig. 25) positions 2, 4, and 5 supported weak vhf signals, and as indicated in Table 21 positions 2, 3, 4, and 5 showed radio duct gradients. It is estimated that 500 nautical miles of the 1100-nautical-mile flight over water could have supported vhf propagation,

#### Mission 12, Karachi, Pakistan, Local Flight

The Mission 12 flight is one of the most remarkable of those made on the trip around the world from the standpoint of vhf propagation conditions. The triangular flight pattern (Fig. 26) originated in Karachi, progressed south southwestward over the Arabian Sea to  $17^{\circ}\text{N}$ ,  $64^{\circ}20'\text{E}$  (450 nautical miles from Karachi and 420 nautical miles from Bombay), then eastward to  $16^{\circ}50'\text{N}$ ,  $70^{\circ}55'\text{E}$  (480 nautical miles from Karachi and 120 nautical miles from Bombay) and then returned northwestward to Karachi.

Both the Karachi and Ahmadabad soundings (Fig. 27) give a good picture of the air mass structure. Both soundings show a continental tropical air mass undergoing tremendous moistening in the surface layers as the air mass drifts in an anticyclonic circulation off the continent over the Arabian Sea. The Karachi sounding shows a specific humidity of 13 grams per kilogram at the surface, decreasing to 7.4 grams per kilogram at 350 feet. The surface layer is very unstable, but from 350 feet to 4900 feet the sounding curve cuts many potential temperature surfaces, which means that the air is very stable. The moisture content of this stable layer is about constant at 8 grams per kilogram. The Ahmadabad sounding shows a specific humidity of 26.5 grams per kilogram at the 350-foot level.



Table 21  
Summary of Mission 11

Position Number	Sounding or Probe	N-break (N-units)	dN 1000 ft	Layer		Temperature		dT 1000 ft	Layer		Distance (naut mi)	Time (Z)
				Top (ft)	Base (ft)	Top (°C)	Base (°C)		Top (ft)	Base (ft)		
1	Sounding	15	- 75	6300	6100	+14.5	+14.5	0.0	6300	6100	50	0125
2	Sounding	45	-129	1950	1600	+20.8	+19.8	+2.9	1950	1600	1014	0635
3	Probe	45	- 90	1700	1200	+20.5	+20.3	+4.0	1700	1200	1040	0645
4	Sounding	48	-240	2200	2000	+20.5	+19.2	+6.5	2200	2000	1068	0653
5	Sounding	36	-144	2600	2350	+20.5	+18.5	+8.0	2600	2350	1130	0710

Table 22  
Refractive Index Gradients

Bangkok, Thailand, 00Z, February 26, 1962		Calcutta, India, 00Z, February 26, 1962	
Layer (10 <sup>3</sup> ft)	dN/dh	Layer (10 <sup>3</sup> ft)	dN/dh
9.90 to 8.00	-20	9.90 to 4.80	- 8
8.00 to 4.80	-10	4.80 to 0.35	-15
4.80 to 4.20	-35		
4.20 to 0.40	-12		
0.40 to 0.35	+25		
0.35 to 0.00	-10		

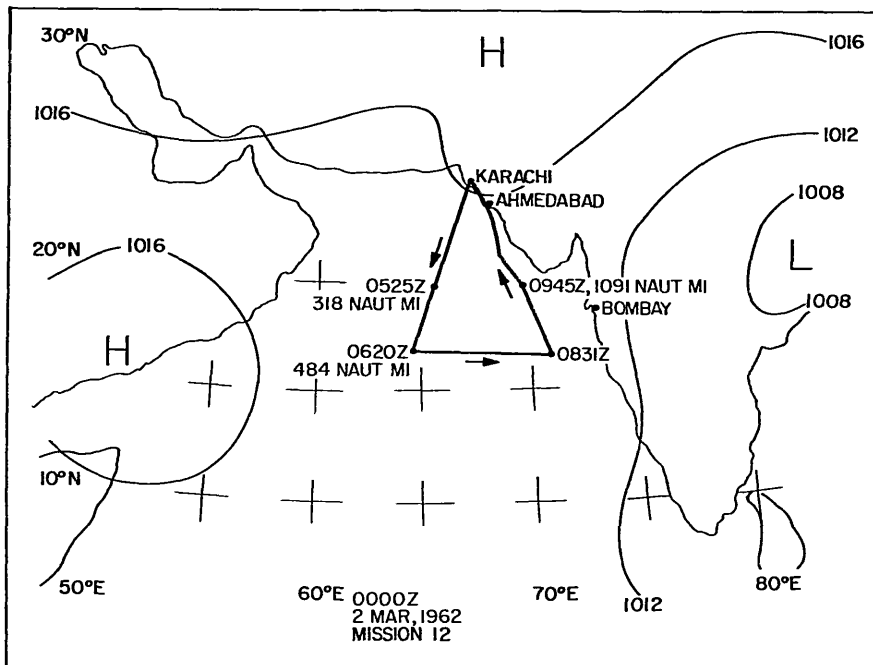


Fig. 26 - Sea-level pressure chart for the area covered in the flight from Karachi, Pakistan (Mission 12)

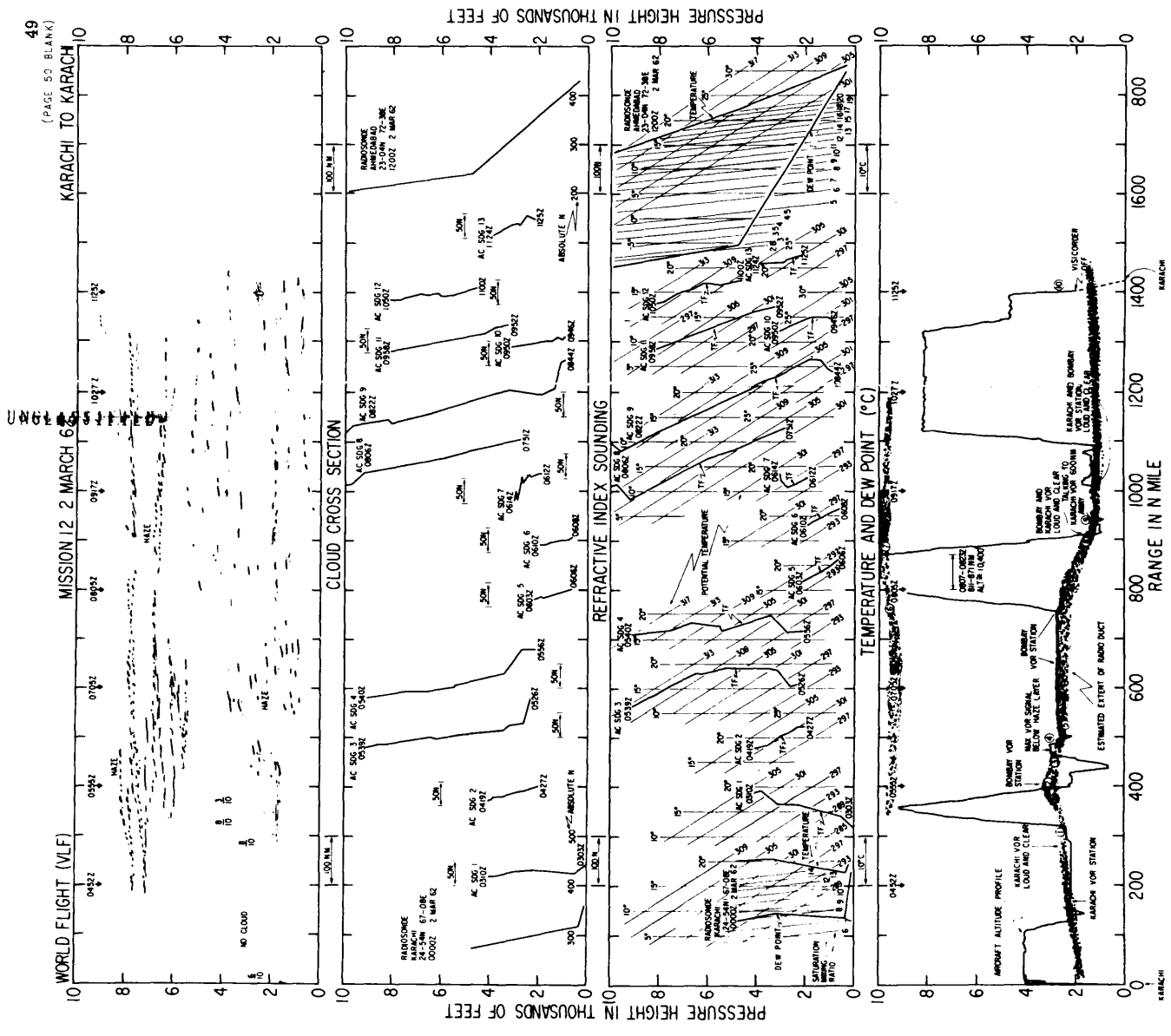


Fig. 27 - Cross section of meteorological conditions in the flight from Karachi, Pakistan (Mission 12)

Table 23  
Summary of Mission 12

Position Number	Sounding or Probe	N-break (N-units)	dN 1000 ft	Layer		Temperature		dT 1000 ft	Layer		Distance (naut mi)	Time (Z)
				Top (ft)	Base (ft)	Top (°C)	Base (°C)		Top (ft)	Base (ft)		
1	Sounding	51	-204	2600	2350	+15.2	+15.5	- 1.0	2600	2300	337	0533
2	Sounding	47	- 67	3400	2700	+19.8	+16.3	+ 5.0	3400	2700	391	0551
3	Sounding	48	-160	3000	2700	+18.5	+16.0	+ 8.3	3000	2700	459	0613
4	Probe	23	-230	2800	2700	+19.0	+19.0	0.0	2800	2700	496	0625
5	Probe	21	-140	2650	2500	+18.3	+17.9	+ 2.7	2650	2500	504	0628
6	Sounding	24	- 48	9700	9200	+11.5	+ 8.5	+ 6.0	9700	9200	811	0807
7	Sounding	24	- 48	10200	9700	+10.9	+ 8.0	+ 5.8	10200	9700	892	0803
8	Sounding	51	-170	1400	1100	+26.4	+24.5	+ 6.3	1400	1100	905	0804
9	Probe	30	-300	1300	1200	+24.5	+23.0	+15.0	1300	1200	944	0857
10	Sounding	20	- 67	2800	2500	+21.5	+22.0	- 1.7	2800	2500	1400	1125

Table 24  
Refractive Index Gradients

Karachi, Pakistan, 00Z, March 2, 1962		Ahmedabad, India, 00Z, March 2, 1962	
Layer (10 <sup>3</sup> ft)	dN/dh	Layer (10 <sup>3</sup> ft)	dN/dh
4.90 to 3.25	- 10	9.90 to 4.80	- 4
3.25 to 2.90	- 6	4.80 to 0.35	-35
0.35 to 0.25	-135		

The moisture then drops off rapidly to 3.0 grams per kilogram at 4800 feet. The lower layer is nearly constant in potential temperature, which means that it is unstable, but from 4800 feet to 9900 feet the specific humidity is nearly constant at about 2.5 grams per kilogram and the potential temperature increases from 309° to 317°K, thus indicating very stable air. For the surface layers mentioned here, the Karachi -135 N/1000-foot soundings (Table 24) show a relatively dry, very stable layer of air which overlays a warm moist surface, the Arabian Sea. This creates an ideal setup for radio duct formation, if the dry air is subsiding over the moist layer.

The weather map (Fig. 26) shows a very flat pressure field, which would indicate divergence or subsidence. The presence of subsidence is also indicated by the extensive haze layers shown on the cloud cross section (Fig. 27). At about 2000 feet the tops of the convective clouds were stopped by a strong temperature inversion lid. Points 1, 2, 3, 4, 5, 8, and 9 of Table 23 of the flight profile (Fig. 27) show the stable temperature inversion in this low-level layer, and the refractive index gradients show strong radio duct layers.

Not only do the refractive index gradients substantiate radio duct formation but both the Karachi and Bombay VOR navigation stations were heard at 112.1 and 112.5 Mc respectively. This shows that this layer was homogeneous and covered an area greater than that shown by the flight path.

This flight is also remarkable in that an upper level radio duct layer was observed. It is hard to chart the top of a haze layer, when the flight does not get at least 1000 feet above it, but the refractive index gradients at points 6 and 7 of Table 23 (and Fig. 27) show a radio duct, and the temperature inversions are strong and indicate that the moisture would be trapped at this layer. The cloud diagram does not show cumulus clouds which could penetrate to this level to supply moisture, but undoubtedly cumulonimbus buildups over land carried moisture to this layer on the afternoon of the previous day and then dissipated.

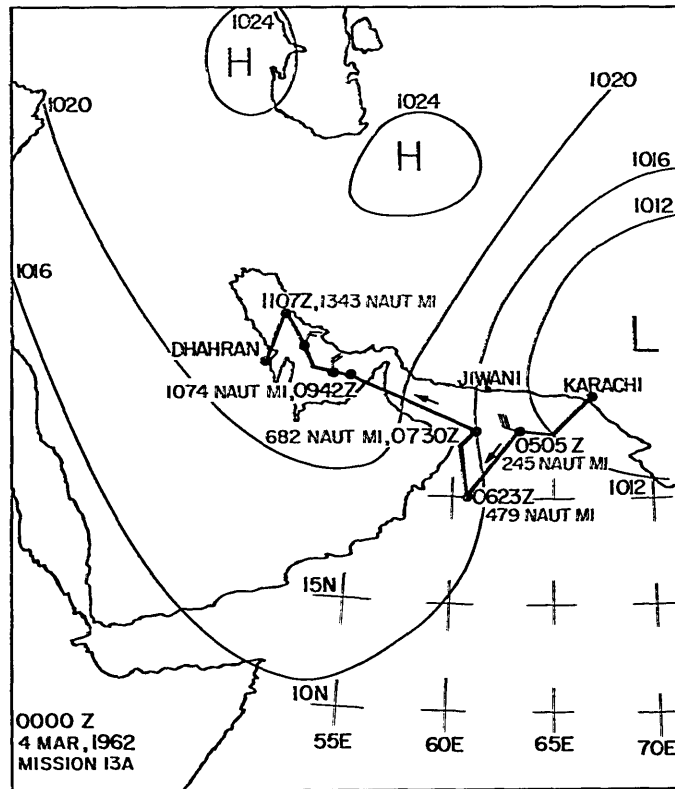


Fig. 28 - Sea-level pressure chart for the area covered in the flight from Karachi, Pakistan, to Dhahran, Arabia (Mission 13A)

In contrast to the strong radio duct layers or super-standard layers observed on this mission there were some substandard layers (which curve radio rays upward into space) observed at about 500 to 3500 feet in aircraft sounding 1 (Fig. 27), 3800 to 4000 feet in aircraft sounding 2, 6100 to 6300 feet in aircraft sounding 3, 6300 to 7300 feet in aircraft sounding 4, 1800 to 1900 feet in aircraft sounding 5, 1900 to 2000 feet in aircraft sounding 6, several sharp shallow layers in aircraft sounding 7, 1500 to 3000 feet and 8200 to 8400 feet in aircraft sounding 9, 900 to 1000 feet in aircraft sounding 10, 5800 to 5900 feet, 6000 to 6200 feet, and 7700 to 7900 feet in aircraft sounding 12, and in a very shallow layer at 2400 to 2500 feet and at 1900 to 2200 feet in aircraft sounding 13. The super-standard and substandard layers are sandwiched together in a complex.

On this basis of the reception of vhf signals from VOR navigation stations when the aircraft was more than 400 nautical miles from either Karachi or Bombay, and on the refractive index gradients shown in Table 23, it is estimated that radio duct conditions were present for 100% of the 1400 nautical miles flown on this mission.

Mission 13A, Karachi, Pakistan, to Dhahran, Saudi Arabia, and  
Mission 13B, Dhahran, Saudi Arabia, to Nicosia, Cyprus

Mission 13A left Karachi and progressed southwestward over the Arabian Sea to 20°10'N, 60°40'E and then generally northward to 23°20'N, 61°00'E; from thence it entered the Gulf of Oman, crossed a narrow peninsula into the Persian Gulf, and arrived at Dhahran (Fig. 28). At most southerly points in this flight the aircraft was 300 nautical miles from the Asian mainland. Over the Gulf of Oman and the Persian Gulf the course was less than 60 nautical miles from land at all times.



Table 25  
Summary of Mission 13A

Position Number	Sounding or Probe	N-break (N-units)	dN 1000 ft	Layer		Temperature		dT 1000 ft	Layer		Distance (naut mi)	Time (Z)
				Top (ft)	Base (ft)	Top (°C)	Base (°C)		Top (ft)	Base (ft)		
1	Sounding	39	- 98	1900	1500	+21.7	+19.3	+ 6.0	1900	1500	5	0313
2	Sounding	24	- 60	2800	2400	+22.0	+22.2	- 0.5	2800	2400	285	0519
3	Sounding	30	- 75	1050	650	+23.5	+23.0	+ 1.2	1050	650	302	0525
4	Sounding	23	- 51	6200	5750	+15.0	+15.0	0.0	6200	5750	340	0537
5	Sounding	17	- 68	7450	7200	+13.0	+13.2	- 0.8	7450	7200	380	0550
6	Probe	15	-150	6600	6500	+11.4	+ 9.8	+16.0	6600	6500	958	0900
7	Sounding	25	- 83	1050	750	+18.9	+18.4	+ 1.7	1050	750	1246	1037
8	Sounding	33	- 73	1100	650	+19.0	+18.5	+ 1.1	1100	650	1274	1046
9	Sounding	15	-100	2300	2150	+17.8	+17.3	+ 3.3	2300	2150	1431	1134

The 0000Z radiosonde curve for Karachi, Pakistan (Fig. 29), shows that the continental tropical air mass is undergoing considerable modification in the lower layers when it is compared with the sounding for the previous day (Fig. 27). Although the potential temperature remained near 292° to 295°K, the specific humidity increased from 7.4 to 12.9 grams per kilogram at the 350-foot (1000-mb) level. There is still an unstable layer near the ground, overlaid by a relatively dry stable layer above.

Table 26  
Refractive Index Gradients  
Karachi, Pakistan, 00Z,  
March 3, 1962

Layer (10 <sup>3</sup> ft)	dN/dh
9.90 to 4.80	- 6
4.80 to 3.25	-20
3.25 to 0.35	-15
0.35 to 0.10	-50

The aircraft measurements (Fig. 29) indicated three ducts over the Arabian Sea. Points 1 and 2 of the flight profile and of Table 25 show the position and strength of the first duct. Although the Jiwani VOR navigation station was heard, it was believed that the aircraft was flying above the radio horizon and the signals would have been heard whether radio duct formation was present or not.

The second duct was observed at position 3 (Table 25). This layer was in accordance with the duct formation indicated by the Karachi radiosonde observation. A bank of cumulus cloud tops was forming below the temperature inversion of +1.2°C/1000 feet as indicated at point 3. The extent of this duct is not known, but it probably is greater than that shown in Fig. 29.

The third duct was observed at 6000 feet at the top of a haze layer. Point 4 of Table 25 shows a refractive index gradient of -51 N-units/1000 feet and an isothermal temperature gradient. Point 5 of the table shows another radio duct layer, but this was not observed on the ascent, so it was not considered of importance. The Jiwani VOR navigation station (113.9 Mc) was heard for considerable time while the aircraft was at least 300 nautical miles away and below the radio horizon at the level of the third duct. This duct was lost when the aircraft ascended for a sounding at the entrance to the Gulf of Oman.

Except for point 6 in Table 25 no radio duct was observed over the Gulf of Oman, but over the Persian Gulf a low-level duct was found as indicated by points 7, 8, and 9 of Table 25 and Fig. 29.

The weather map (Fig. 28) shows a general flow of dry continental air over the entire route. From the north-to-south flow and the isobaric curvature one would expect divergence to be increasing generally. The flight measurements show that radio duct formation was present except where there was not sufficient moisture in the lower layers to create a dry/moist air interface.

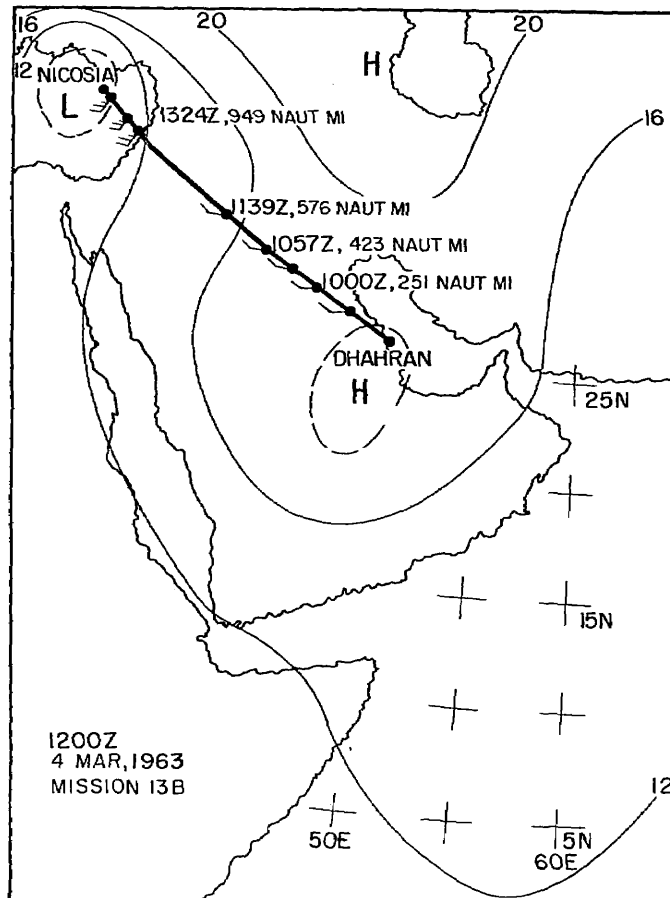


Fig. 30 - Sea-level pressure chart for the area covered in the flight from Dhahran, Arabia, to Nicosia, Cyprus (Mission 13B)

It is estimated that about two-thirds of the 1450 nautical miles of this flight was favorable for radio duct formation.

The flight from Dhahran to Nicosia (Fig. 30) was conducted on the next day. Instead of being in an anticyclonic circulation, the circulation changed to cyclonic, a low centered over Nicosia in the Mediterranean Sea. An indication of radio duct formation was present over Dhahran, point 1 of Mission 13B (Fig. 31). As soon as the flight progressed inland this layer was lost.

On this flight radio duct formation was not indicated because (a) no subsidence was indicated by the weather map over the Mediterranean Sea, and in accordance with Eqs. (2), (3), and (9) conditions would be unfavorable for the creation of dry/moist air interfaces, and (b) the flight over the Arabian desert did not have a moisture source region beneath to create and sustain a dry/moist air interface in the regions even if Eqs. (2), (4), (8), and (9) might have shown increasing stratification.

#### Mission 14, Nicosia, Cyprus, to Rota, Spain

One would expect the landlocked Mediterranean Sea to be an ideal spot for radio duct formation. Most of the air mass currents that reach this body of water have had a trajectory over land. The air mass should be dry in the lower layers, and then upon passing

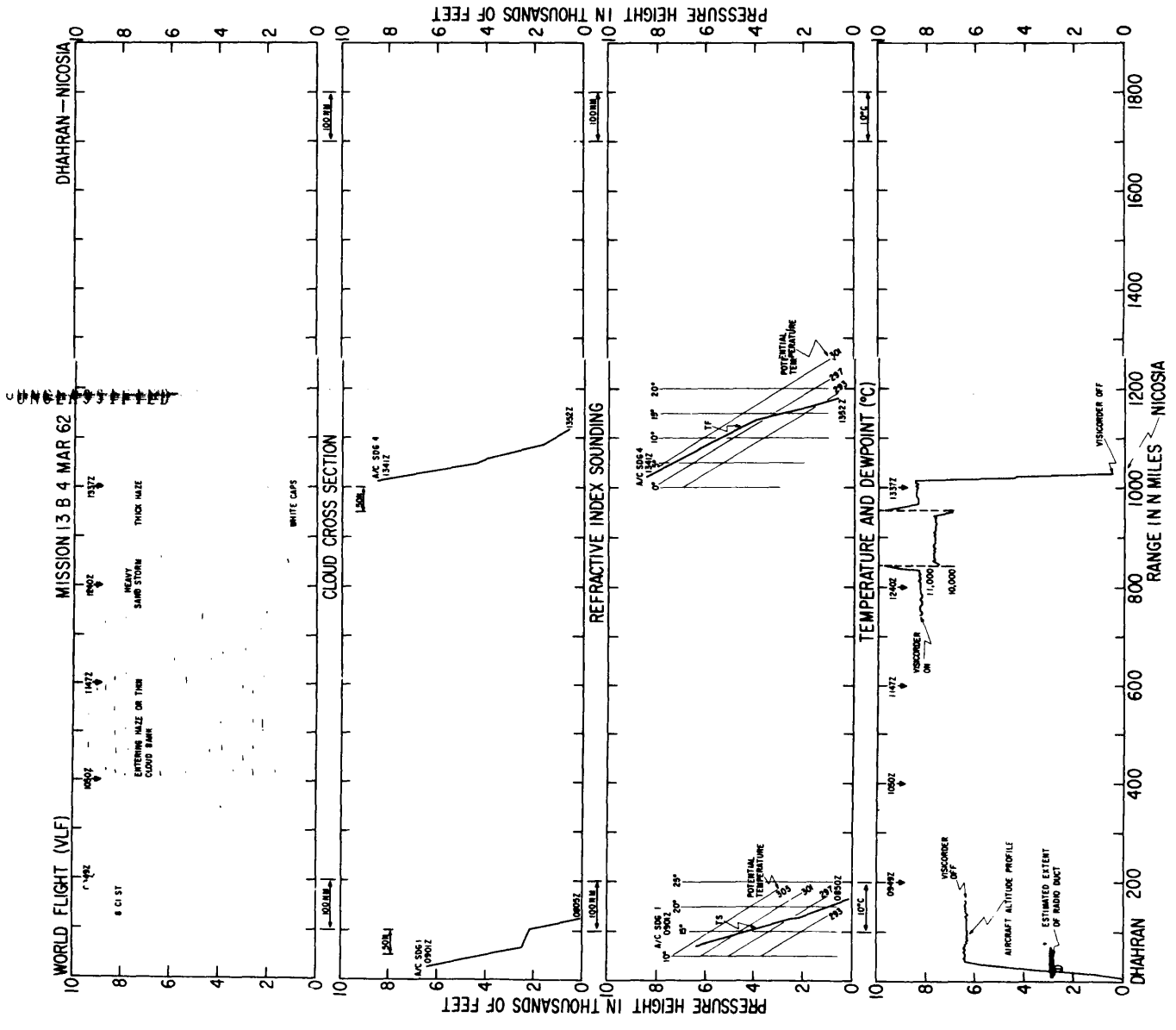


Fig. 31 - Cross section of meteorological conditions in the flight from Dhahran, Arabia, to Nicosia, Cyprus (Mission 13B)

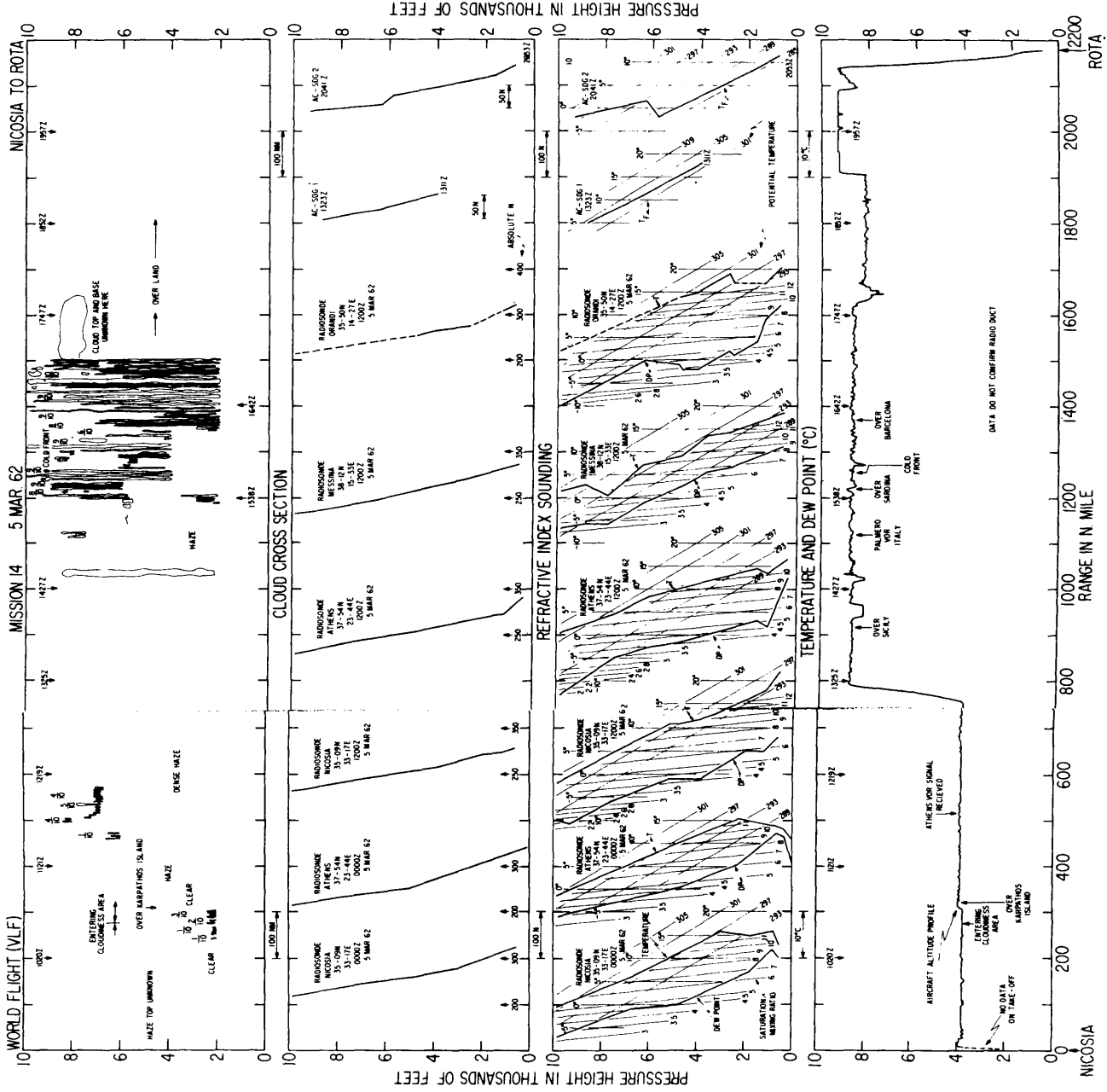


Fig. 32 - Cross section of meteorological conditions in the flight from Nicosia, Cyprus, to Rota, Spain (Mission 14)

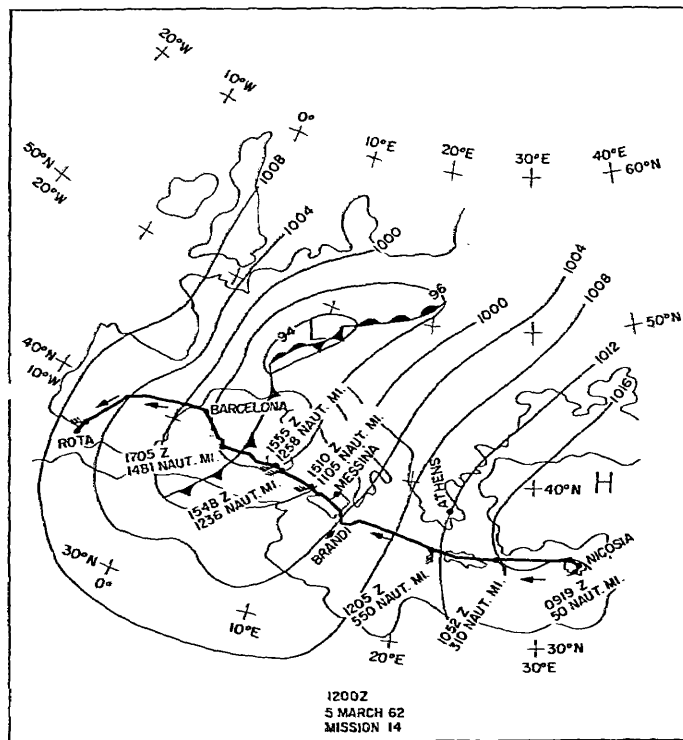


Fig. 33 - Sea-level pressure chart for the area covered in the flight from Nicosia, Cyprus, to Rota, Spain (Mission 14)

over the water surface a moisture gradient at the surface should be created which would support radio duct formation. The only sounding which supports this conclusion is the Athens 12Z radiosonde observation for March 5, 1962 (Fig. 32). The radiosonde observation shows a refractive index gradient of  $-50$  N-units/1000 feet for the layer up to 1200 feet above the surface. The other radiosonde observations do not show radio duct formation on the radiosonde observation N-curves.

The radiosonde curves (Fig. 32) show dry air of the continental polar type undergoing moistening in the lower layers, but for the exception of Athens there is not a sufficient moisture gradient to produce the required  $-48.6$  N-units/1000 feet required to sustain a radio duct.

This situation is a good illustration of the principles stated in Eqs. (2), (4), (8), and (9) when the weather map (Fig. 33) is considered with the soundings. With the exception of Nicosia there is convergence, since the air mass current has a south-to-north flow and the isobars are becoming more cyclonically curved as the cold front is approached between Spain and Sardinia. Although moisture is added to the surface layer of air, the lapse rate is decreasing, which means that the moisture is not trapped sufficiently to produce a sharp dry/moist air-layer interface. The air approaching Athens has had a longer trajectory over the water, consequently the moisture gradient is steeper, since the specific humidity is 10 grams per kilogram at the surface. This is a greater value than that shown at any of the other Mediterranean stations. One would expect the same to be true at Nicosia, but here the lower layer has not been moistened by a long trajectory over water, as shown by the fact that the specific humidity is only 6.6 grams per kilogram.

Table 27  
Summary of Mission 14

The data do not confirm a radio duct

Table 28  
Refractive Index Gradients

Nicosia, Cyprus, 12Z, March 5, 1962		Athens, Greece, 12Z, March 5, 1962		Messina, Sicily, 12Z, March 5, 1962	
Layer (10 <sup>3</sup> ft)	dN/dh	Layer (10 <sup>3</sup> ft)	dN/dh	Layer (10 <sup>3</sup> ft)	dN/dh
9.40 to 5.10	-15	9.90 to 7.60	-12	9.90 to 8.80	-11
5.10 to 4.80	-15	7.60 to 6.10	- 7	8.80 to 7.90	-11
4.80 to 3.85	-10	6.10 to 4.80	- 7	7.90 to 6.40	-11
3.85 to 3.20	-15	4.80 to 1.60	- 7	6.40 to 3.80	-11
3.20 to 1.95	-15	1.60 to 1.20	-23	3.80 to 2.80	-12
1.95 to 1.20	-15	1.20 to 0.35	-54	2.80 to 0.50	-13
1.20 to 0.40	-18	0.35 to 0.00	-44		

No radio duct formation was indicated in Fig. 32, or in Tables 27 and 28, for the flight profile. The low-level duct indicated at Athens was considerably north of our path and was not regarded as a radio duct along the flight path (Fig. 33).

This flight is a good example of the effect of the weather map indications of air mass trajectory and motion on radio duct formation. If a high-pressure area had been centered over the Mediterranean Sea with the air mass flow from north to south over the water so that there would have been divergence with vertical subsidence, then conditions would have been more favorable for radio duct formation.

#### Mission 15, West Malling, England, to Keflavik, Iceland

The flight path from West Malling to Keflavik is across a deepening col joining two low centers located at 55°N, 25°W, and 67°N, 10°E having pressures at their centers of 996 mb and 1008 mb respectively (Fig. 34). The weather map shows cyclonic curvature of the isobars except for about 300 nautical miles from Keflavik. In accordance with Eqs. (2) and (3) one would not expect this to be a region of radio duct formation, since the absolute vorticity would be increasing as the aircraft progressed northward. However, by the same equations when the isobaric curvature changes from cyclonic to anti-cyclonic at about 300 nautical miles from Keflavik, one might expect to find the divergence and conditions more favorable for duct formation.

The radiosonde curves for West Malling, Valentia, and Keflavik shown in Fig. 35 indicates values of specific humidity and potential temperature typical of a polar continental air mass. At all stations the specific humidity is less than 4 grams per kilogram, and the potential temperatures vary from 270° to 370°K. The radiosonde curves for this flight show no tendency toward duct formation (Fig. 35 and Table 28), but the aircraft sounding at Keflavik (aircraft sounding 4) shows a sharp refractive index gradient with an N-break which is less than the arbitrary choice of 15 N-units required for radio duct formation. This is indicative of subsidence taking place as indicated by the divergence shown in the pressure field.

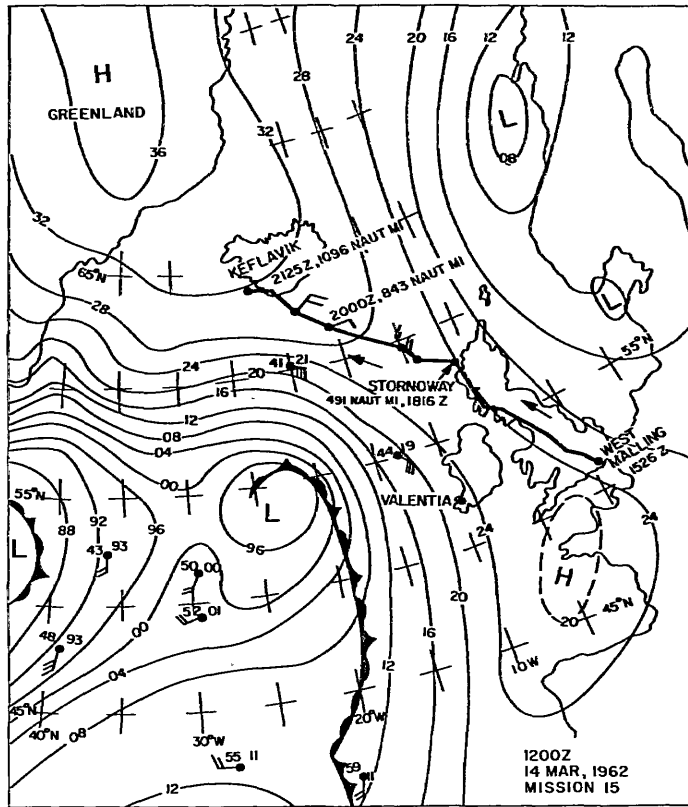


Fig. 34 - Sea-level pressure chart for the area covered in the flight from West Malling, England, to Keflavik, Iceland (Mission 15)

Table 29  
Summary of Mission 15

The data do not confirm a radio duct

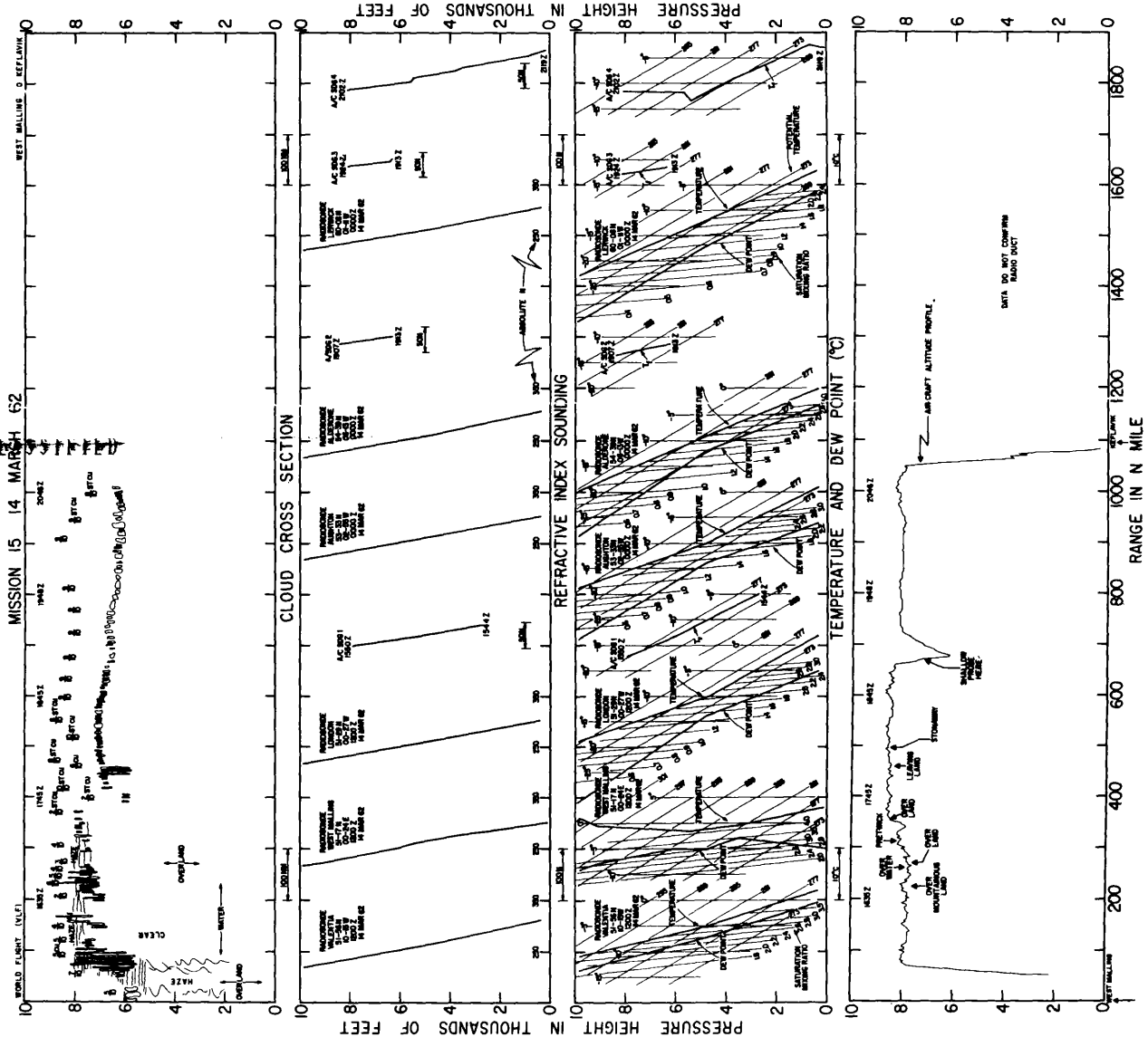


Fig. 35 - Cross section of meteorological conditions in the flight from West Malling, England, to Keflavik, Iceland (Mission 15)

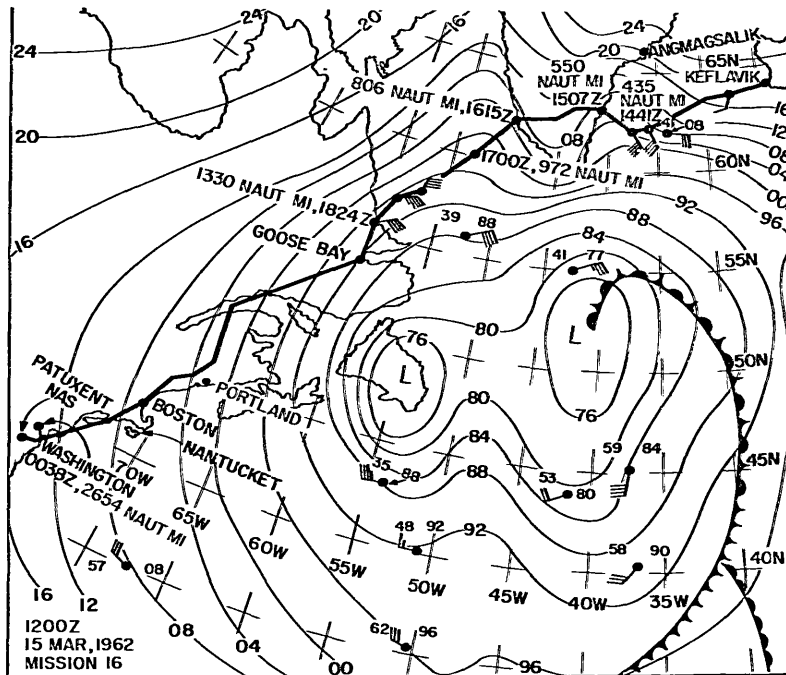


Fig. 36 - Sea-level pressure chart for the area covered in the flight from Keflavik, Iceland, to Patuxent, Maryland (Mission 16)

#### Mission 16, Keflavik, Iceland, to Patuxent NAS, Maryland

The flight from Keflavik to Patuxent was on the periphery of an occluding cyclonic system having two centers, one over Newfoundland and the other at  $53^{\circ}\text{N}$ ,  $41^{\circ}\text{W}$  (Fig. 36). Both centers had pressures of 976 mb at their centers. Strong to gale tail winds were experienced over most of the overwater portion of the flight. The flight path was from Keflavik to Greenland over the ice cap at Greenland about latitude  $63^{\circ}\text{N}$ , across Davis Strait to Goose Bay, and then down the Atlantic Coast to Patuxent NAS.

Pronounced orographic effects were noticeable while crossing Greenland. The broken lower clouds observed from 1349Z to 1500Z after leaving Keflavik became a solid bank as the moist air was forced up the ice cap to the continental divide. After crossing the ridge of the ice cap the clouds broke with the downslope winds. The ice cap was visible at the summit and afterward until about 150 nautical miles off the western coast of Greenland. Another cloud bank was encountered over Davis Strait and continued until the aircraft was over North America.

The orographic effect produced by the upslope and downslope winds passing over the ice cap is similar to the effect of convergence and divergence in the free atmosphere (Fig. 37). In the ascending current of air, the moisture is cooled to its dew point and a constant cloud layer is observed as long as the ascending currents exist, but with the downslope wind the air is adiabatically heated and dried (foehn effect) and the clouds disappear.

It was impossible to make temperature and refractive index measurements while observing these interesting effects because shortly after leaving Keflavik the instrument sensors became encrusted in a cake of ice and remained so covered until reaching North America. However, considerable information can be judged from the radiosonde

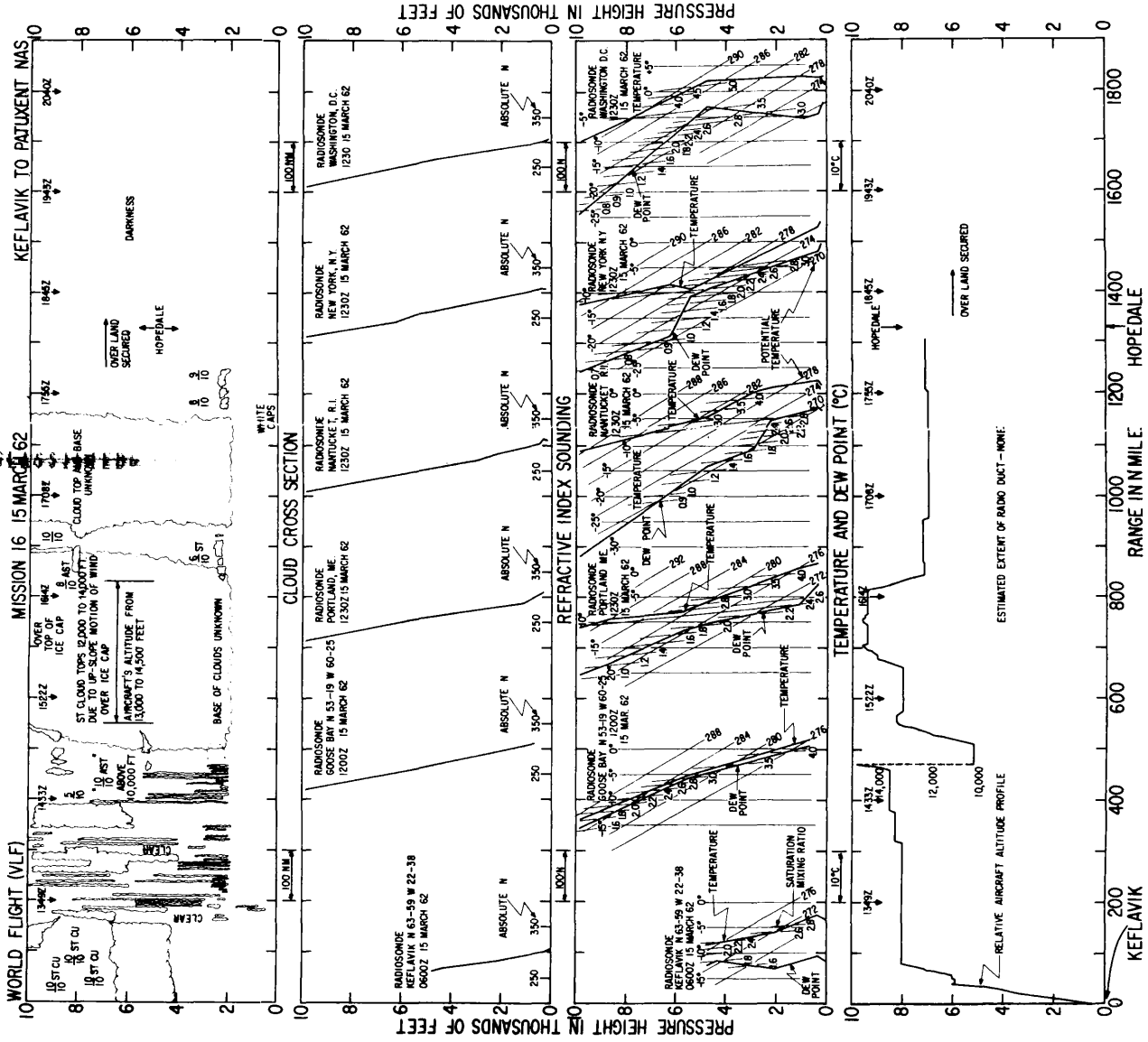


Fig. 37 - Cross section of meteorological conditions in the flight from Keflavik, Iceland, to Patuxent, Maryland (Mission 16)

Table 30  
Refractive Index Gradients

West Malling, England, 12Z, March 14, 1962		Valentia, Ireland, 12Z, March 14, 1962		Keflavik, Iceland, 06Z, March 15, 1962	
Layer (10 <sup>3</sup> ft)	dN/dh	Layer (10 <sup>3</sup> ft)	dN/dh	Layer (10 <sup>3</sup> ft)	dN/dh
9.90 to 9.15	- 5	9.90 to 4.80	- 5	4.80 to 4.30	-20
9.15 to 6.05	- 9	4.80 to 0.35	-10	4.30 to 2.10	- 5
6.05 to 5.40	- 9			2.10 to 0.35	-10
5.40 to 4.80	-15			0.35 to 0.00	-34
4.80 to 3.55	-12				
3.55 to 0.10	-15				

Table 31  
Summary of Mission 16

The data do not confirm a radio duct

Table 32  
Refractive Index Gradients

Keflavik, Iceland, 06Z, March 15, 1962		Goose Bay, Nfld., 12Z, March 15, 1962		Portland, Me., 12Z, March 15, 1962		Washington, D.C. 12Z, March 15, 1962	
Layer (10 <sup>3</sup> ft)	dN/dh	Layer (10 <sup>3</sup> ft)	dN/dh	Layer (10 <sup>3</sup> ft)	dN/dh	Layer (10 <sup>3</sup> ft)	dN/dh
4.80 to 4.30	-20	9.90 to 4.80	-8	9.90 to 9.00	- 6	9.90 to 4.80	- 8
4.30 to 2.10	- 5	4.80 to 0.35	-8	9.00 to 4.80	- 6	4.80 to 1.00	- 8
2.10 to 0.35	-10			4.80 to 1.00	- 5	1.00 to 0.35	-25
0.35 to 0.00	-34			1.00 to 0.35	-28	0.35 to 0.00	-36

observations as shown in Fig. 37. None of the soundings shows refractive index gradients sufficient to produce radio duct formation (Tables 30, 31, and 32).

These soundings show the characteristics of a polar continental air mass relatively low values of potential temperature and specific humidity. The Keflavik sounding shows extremely low specific humidities, less than 2 grams per kilogram at all levels, and very low potential temperatures in the lower 5000 feet of the sounding, less than 280°K. At Goose Bay (Fig. 36) the polar continental air mass curve shows some modification. The specific humidity at 350 feet (1000 mb) has increased to 4 grams per kilogram (Fig. 37) and the potential temperature at this level has increased from 268°K at Keflavik to 277°K at Goose Bay. Portland shows little modification over Goose Bay in the lower levels, but the potential temperature at 9900 feet (700 mb) has increased from 285° to 290°K. The Washington, D.C., sounding shows an influx of moister and potentially warmer air at the 4800-foot (850 mb) level. None of these soundings show refractive index gradients which would support radio duct formation (-48.6 N-units/1000 feet or less).

It is important to mention here that polar continental air reaching Portland had a trajectory from Keflavik, since the soundings at the two stations show nearly the same conservative air mass properties. In accordance with the theory expressed by Eqs. (2), (3), and (4), if radio duct formation were not present at the gradient level at Portland, it would not be observed at any point north of this point along the parcel trajectory. This is certainly verified in this case. The Washington, D.C., sounding can not be compared

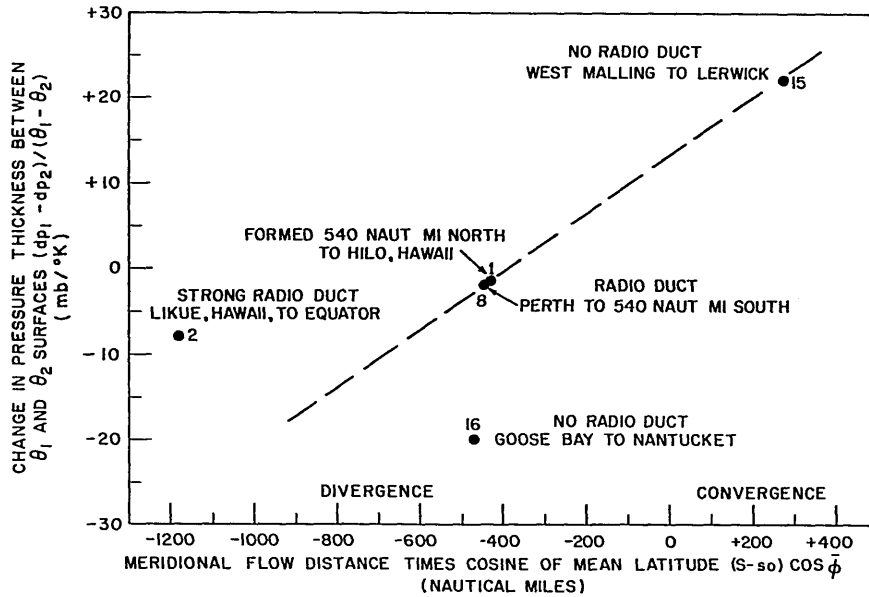


Fig. 38 - Change in pressure thickness with latitude

with the Keflavik, Goose Bay, and Portland soundings, because the air moving over Washington, D.C., had a much different trajectory.

## CONCLUSIONS

The experimental results measured during the around-the-world trip seem to confirm the theory set forth in this report about radio duct formation at vhf and uhf. While many more measurements are necessary to improve the techniques used, the results are encouraging.

For the case of meridional flow direct substitutions were made from the meteorological soundings into Eq. (8) for Missions 1, 2, 8, 15, and 16. The results were plotted in Fig. 38. This figure shows a gross correlation between the component of distance traveled by an air parcel stream along a meridian, and the change in the pressure thickness of the parcels at the original and final positions of the measurement. It is argued from this figure and the related data that:

1. Radio ducts are continuous in a broad stream of air flowing toward the equator if they are observed originally in the upstream current (Missions 2 and 8 in Fig. 38)
2. If the radio ducts are not present originally in the upstream current, they will not form in a broad stream of air flowing toward the pole (Missions 15 and 16 in Fig. 38).
3. Even if radio ducts are not observed in the upstream direction, they may be formed later in a broad equatorward-flowing current (Mission 1 in Fig. 38).

Equation (8) could also have been applied in Missions 5, 6, and 14, but data were not available to check these missions because of the flight path.

For the case of refractive index gradients at the center of a pressure system it was possible to observe the 24-hour change in refractive index gradient between two potential-temperature surfaces and to compare it with the 24-hour pressure change on the sea-level

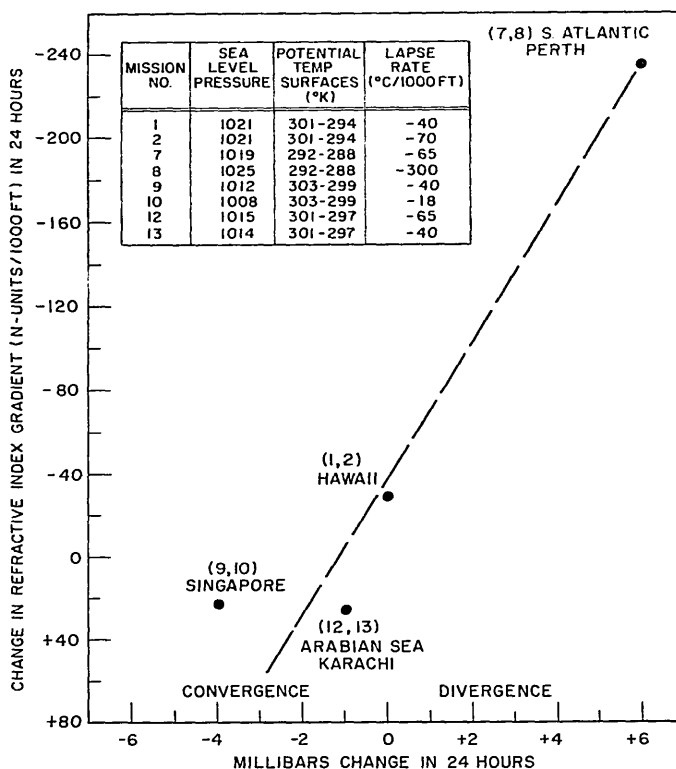


Fig. 39 - Variation of refractive index gradient with 24-hour pressure change

weather chart. These refractive index gradients were selected at levels where radio duct formation had already occurred or was likely to occur. These points are plotted in Fig. 39. There is a gross correlation between the steepening of the refractive index gradients and increasing pressure change at the center of the pressure system. When this principle is applied to radio duct formation, Fig. 39 shows that:

1. Radio ducts, defined by two potential-temperature surfaces, at the top and bottom of a temperature inversion level, continue or strengthen if the pressure increases at the center of the pressure system over 24 hours (Missions 7 and 8 of Fig. 39).

2. Radio ducts, as defined above, do not exist if they are not observed initially and the pressure at the center of the system decreases over a period of 24-hours (Missions 9 and 10 of Fig. 39).

3. A radio duct, as defined above, may be formed in a high-pressure system if the pressure at the center of the system either increases or remains stationary (Missions 1 and 2 of Fig. 39). Conversely, a radio duct may dissipate if the pressure at the center of such a system decreases over 24 hours (Missions 12 and 13 of Fig. 39).

For the case of temperature gradients at the center of a pressure system, 24-hour changes in the temperature gradient between two potential-temperature surfaces were compared with the 24-hour pressure change on the sea-level weather chart. These points are plotted in Fig. 40. Again, there is a gross correlation between increasing 24-hour pressure changes and steepening temperature gradients. A comparison of Figs. 39 and 40 shows that increasing temperature inversions are generally associated with increasing refractive index gradients when the layers are defined as above.

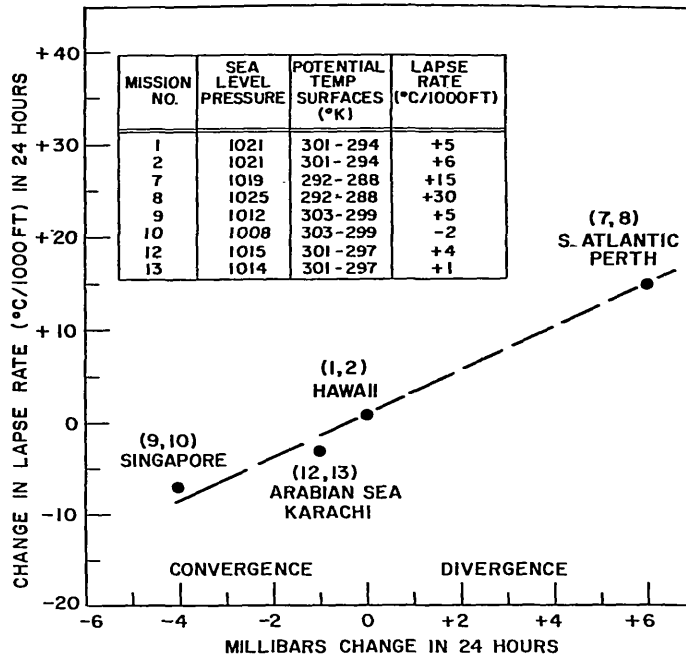


Fig. 40 - Variation in temperature lapse rate with 24-hour pressure change

In confirmation of the principle that increasing pressure is favorable to duct formation and to steepening temperature gradients, it was found that ducts were present in Missions 1, 4, 5, 6, 7, 10, 11, 12, and 13 in those portions of the flight path which lay across the center of an anticyclone or a high-pressure ridge (Table 33). In Missions 1, 2, 3, 4, 6, 8, 9, and 14, portions of the flight path crossed cyclones or low-pressure troughs, and no ducts were observed (Table 34). In these cases, of course, there was present no initial observation to establish the existence or nonexistence of a radio duct, but they do show that if pressure increases long enough over water, highs are formed which have radio ducts, and if pressure falls long enough over water, lows are formed which do not have ducts.

In Table 33 the observations show refractive index gradients of less than  $-48.6$  N-units/1000 feet and associated temperature gradients of more than  $-1.8^{\circ}\text{C}/1000$  feet (the average lapse rate if air is neither sinking nor rising) with two exceptions: In Mission 4 the aircraft was in a high-pressure center, but the observation, point 8, is for a flight through the side of a cloud, not the cloud top at the dry/moist air interface. For point 8 the refractive index gradient and the temperature gradient are out of phase with the other refractive index and temperature gradients in Table 33. The same is true for point 9 of Mission 6. (In both these cases  $dq/dh$  was greater than zero.)

In addition to the predictability of the tendency toward radio duct formation by air-mass mechanical motions and transitions due to the addition or subtraction of moisture, it is interesting to note that there is gross agreement with respect to summer and winter when the 21,720 nautical miles of overwater flight is analyzed further:

1. During winter, north of latitude  $25^{\circ}\text{N}$ , 5050 nautical miles were flown with a radio duct mileage of about 200 nautical miles. Radio duct formation was observed 4% of the distance.

Table 33  
Refractive Index and Temperature Gradients in an Anticyclone

Mission	Pressure at Center or Ridge	Position		Flight Distance (naut mi)	dg/dh ≤ 0			dg/dh ≥ 0				
		Lat.	Long.		Point	dN/dh (N-units/1000 ft)	Point	dt/dh (°C/1000 ft)	Point	dN/dh (N-units/1000 ft)	Point	dt/dh (°C/1000 ft)
1. McChord to Hickam	1021	21 N	158 W	2000 to 2300	5	-78	5	+15.8				
	Meridional flow			1600 to 2300	6	-83	6	+11.7				
2. Hickam to Tafuna				0 to 1900								
4. Nandi to Sydney	1009	25 S	168 E	500 to 900	2 to 7	-150 to -86	2 to 7	+0.7 to +11.0	8	-67	8	-2.3
5. Sydney to Perth	1017	32 S	132 E	600 to 1200	2	-78	2	+4.2				
	Meridional flow			400 to 1050	3	-71	3	+3.2				
6. Perth to Perth	1018	34 S	112 E	0 to 400	1 to 3	-220 to -250	1 to 3	+7.0 to +5.1	9	-190	9	-23.0
	Meridional flow			1050 to 1470	8 and 10	-147 to -230	8 and 10	+10.0 to +12.6				
7. Perth to Perth	1018	37 S	113 E	1126 to 1800	2 to 3	-70 to -70	2 to 3	+18.3 to +14.3				
	Meridional flow			100 to 700	1	-49	1	+12.5				
8. Perth to Perth				0 to 900								
10. Singapore to Bangkok	1008	3 N	103 E	0 to 500	1 to 3	-60 to -152	1 to 3	+6.4 to +3.0				
11. Bangkok to Calcutta	1009	15 N	95 E	165 to 1200	2 to 5	-90 to -144	2 to 5	+2.9 to +8.0				
12. Karachi to Karachi	1015	21 N	68 E	0 to 1200	1 to 10	-49 to -300	1 to 10	-1.7 to +15.0				
13. Karachi to Dhahran	1021	23 N	53 E	0 to 1000								
	Meridional flow			750 to 1400	7 to 9	-73 to -100	7 to 9	+1.1 to +3.3				
15. W. Malling to Keflavik	1028 to 1032	61 to 64 N	15 to 24 W	700 to 1000								
					Radio ducts had not developed							

Table 34  
Refractive Index and Temperature Gradients in a Cyclone

Mission	Pressure at Center or Trough	Position		Flight Distance (naut mi)	$dq/dh \leq 0$			$dq/dh \geq 0$				
		Lat.	Long.		Point	$dN/dh$ (N-units/1000 ft)	Point	$dT/dh$ ( $^{\circ}C/1000$ ft)	Point	$dN/dh$ N-units per 1000 ft	$dT/dh$ ( $^{\circ}C/1000$ ft)	
1. McChord to Hickam	988 984	43 N 39 N	133 W 138 W	0 to 860								
2. Hickam to Tafuna	1009	15 S	170 W	1900 to 2400					11	-240	11	+4.0
3. Tafuna to Nandi	1006	15 to 19 S	170 W to 177 E	0 to 660					1 to 9	-45 to -230	1 to 9	-2.0 to +32.0
4. Nandi to Sydney	1008 1007	21 S 32 S	175 E 156 E	0 to 500 1000 to 1750					1	-150	1	-9.0
6. Perth to Perth	1015	38 S	107 E	500 to 800				None		Frontal zone		
8. Perth to Perth	1020	44 S	113 E	900 to 1000				None		Frontal zone		
9. Perth to Singapore	1008 1007	17 S to 15 S	111 E to 105 E	950 to 1150 1200 to 2200				None		Intertropic front	1	+1.5
14. Nicosia to Rota	995	40 N	3 E	1100 to 1400				None				
15. W. Malling to Keflavik	Meridional flow			0 to 700				None				
16. Keflavik to Patuxent	Meridional flow			1330 to 2200				None				

2. During winter, south of latitude  $25^{\circ}\text{N}$  to the equator, 5920 nautical miles were flown with a radio duct mileage of about 4595 nautical miles. Radio duct formation was observed 78% of the distance.

3. During summer, north of latitude  $25^{\circ}\text{S}$  to the equator, 3600 nautical miles were flown with a radio duct mileage of about 100 nautical miles. Radio duct formation was observed 3% of the distance.

4. During summer, south of latitude  $25^{\circ}\text{S}$ , 7150 nautical miles were flown with a radio duct mileage of about 2900 nautical miles. Radio duct formation was observed 40% of the distance.

It is interesting that radio duct formation conditions would be most prevalent between the equator and  $25^{\circ}\text{N}$  in the winter, and between latitude  $25^{\circ}\text{S}$  and  $45^{\circ}\text{S}$  in the summer. This is an indication that vhf and uhf anomalous radio propagation is a worldwide phenomenon in anticyclonic belts or regions of divergence.

### WORLD DIVERGENCE MAPS

On the basis of this theory and the data collected, mean worldwide wind-pressure maps (8) were marked to show regions where divergence would be most likely to occur at different seasons of the year. These surface maps were representative of the mean flow patterns at the gradient wind level where the radio duct formation process takes place. These maps consisted of the mean sea-level pressure patterns and the prevailing winds associated with these patterns for the months of January, March, May, July, September, and November. Arrows indicated the direction from which the most frequently observed wind blows, and barbs marked the percentage of observations with this prevailing wind direction, with each barb representing 10 percent. The rules for constructing the areas of divergence shown in Fig. 41 from these mean wind-pressure maps are as follows:

1. The isobars in the mean sea-level pressure field must show anticyclonic curvature or include the center of an anticyclone or its associated high-pressure ridge.
2. The wind arrows in these areas must be within  $45^{\circ}$  of equatorward flow, and the indicated winds must be from this direction 30 percent of the time, except at the center of an anticyclone or its associated high-pressure ridge.
3. Equatorial flowing winds in areas of cyclonically curved isobars are excluded.

The maps in Fig. 41 should be useful in pinpointing regions where radio duct formation is likely to occur.

From the summaries of meteorological data in Figs. 38, 39, and 40 and Tables 33 and 34 it was found that radio duct formation conditions would persist over the ocean if a radio duct was originally associated with divergence at or above the gradient wind level under the following conditions: (a) a broad current of moist air flowing toward the equator, with dry air subsiding above it, and having a direction component of  $45^{\circ}$  or less to the meridian, (b) an anticyclone or high-pressure ridge where there is an outward component of air flowing across the isobars, or an increasing pressure at the center of the system, over a 24-hour period, and (c) a temperature lapse rate of  $-1.8^{\circ}\text{C}/1000$  feet or more with increasing temperature gradient with time, or increasing pressure with time at the center of the pressure system, over a 24-hour period. This criterion fails if there is a moist air layer over the marine layer, or if water saturation takes place because of vertical expansion of the parcels above the level of the duct. A good check is to specify that the lapse rate of specific humidity be negative, i.e.,  $dq/dh$  must be less than zero.

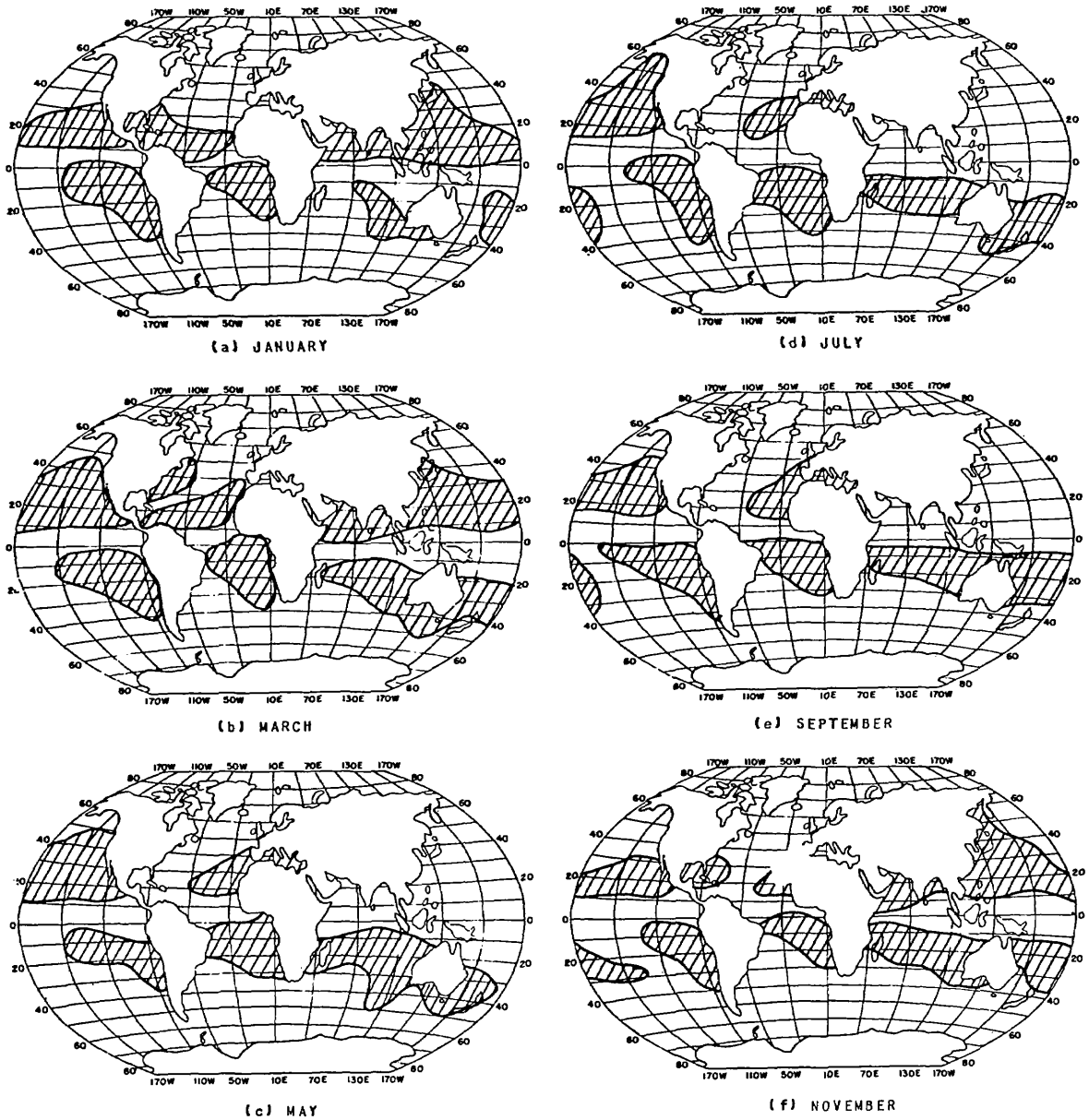


Fig. 41 - World divergence maps, showing areas over the oceans where divergence is likely to occur in the mean air flow patterns. The maps are arranged so that each side-by-side pair shows opposite seasons for the same hemisphere or the same season for opposite hemispheres.

Conversely, radio duct conditions will not persist over the ocean when convergence occurs at or above the gradient level as indicated by: (a) a broad current of air flowing toward the pole and having a direction component of  $45^\circ$  or less to the meridian, (b) a cyclone or a trough of low pressure where there is an inward component of air flowing across the isobars or a decreasing pressure at the center of the system over a 24-hour period, and (c) a temperature lapse rate of less than  $-1.8^\circ\text{C}/1000$  feet and decreasing pressure at the center of the system, or decreasing vertical temperature gradients at the center of the system.

If the reader is interested in making propagation forecasts, the divergence maps should be consulted only as a means of showing probable areas of divergence which would be favorable to radio duct formation. The propagation forecast should be made on the basis of current weather maps, meteorological soundings of pressure, temperature, humidity, and refractive index, and radio or radar observations of ducts.

## REFERENCES

1. Wave Propagation Branch staff, "Meteorological Measurements in the South Atlantic," Report of NRL Progress, June 1960, pp. 1-13
2. D.L. Ringwalt and F.C. Macdonald, "Elevated Duct Propagation in the Tradewinds," IRE Trans. AP-9:377 (July 1961)
3. Wave Propagation Branch staff, "The Elevated Duct Between San Diego and Hawaii," Report of NRL Progress, Apr. 1961
- 4a. (Report I) "Synopsis of December 1960 Flight of Project Tradewinds IV," NRL letter report 5270-32, Aug. 23, 1961
- 4b. (Report II) "Synopsis of January 1961 Flight of Project Tradewinds IV," NRL letter report 5270-33, Aug. 23, 1961
- 4c. (Report III) "Synopsis of February 1961 Flight of Project Tradewinds IV," NRL letter report 5270-34, Aug. 23, 1961
- 4d. (Report IV) "Synopsis of March 1961 Flight of Project Tradewinds IV," NRL letter report 5270-50, Oct. 4, 1961
- 4e. (Report V) "Synopsis of April 1961 Flight of Project Tradewinds IV," NRL letter report 5270-6A, Oct. 4, 1961
- 4f. C.G. Purves, "A Month-By-Month Study of the Elevated Duct Between San Diego and Hawaii (Project Tradewinds IV), VI. Synopsis of June 10-13, 1961 Flight," NRL Memorandum Report 1365, Oct. 8, 1962
- 4g. D.L. Randall (Report VII) "Project Tradewinds IV: Radiometeorological Conditions in the Elevated Duct Between San Diego and Honolulu (June 22 and 26, 1961)," Report of NRL Progress, May 1962
- 4h. C.G. Purves, "A Month-By-Month Study of the Elevated Duct Between San Diego and Hawaii (Project Tradewinds IV), VIII. Synopsis of July 18-21, 1961 Flight," NRL Memorandum Report 1367, Oct. 18, 1962
- 4i. C.G. Purves, "A Month-By-Month Study of the Elevated Duct Between San Diego and Hawaii (Project Tradewinds IV), IX. Synopsis of August 21-26, 1961 Flight," NRL Memorandum Report 1416, Apr. 3, 1963
- 4j. D.F. Hemenway and D.L. Randall, "Radar Meteorological Observations of an Elevated Duct" (Project Tradewinds IV: Report X - Synopsis of September 26-30, 1961, Flight), Report of NRL Progress, June 1962
- 4k. C.G. Purves, "A Month-By-Month Study of the Elevated Duct Between San Diego and Hawaii (Project Tradewinds IV), XI. Synopsis of October 10-13, 1961 Flight," NRL Memorandum Report 1437, June 26, 1963

41. C.G. Purves, "A Month-By-Month Study of the Elevated Duct Between San Diego and Hawaii (Project Tradewinds IV), XII. Synopsis of 28 November - 2 December, 1961 Flight," NRL Memorandum Report 1453, Sept. 1963
5. H.A. Panofsky, "Introduction to Dynamic Meteorology," the Pennsylvania State University Press, 1958, pp. 39-45 and 108-124
6. S. Petterssen, "Weather Analysis and Forecasting," 2nd edition, vol. 1, New York: McGraw-Hill, 1956
7. H.R. Reed and C.M. Russell, "Ultra High Frequency Propagation," New York: Wiley, 1953, pp. 42-57
8. F.A. Berry, Jr., E. Bollay, and N.R. Beers, editors, "Handbook of Meteorology," New York: McGraw-Hill, 1945. Divergence maps were constructed from figures on pages 939, 940, 941, 943, and 944; used by permission of the publisher.

#### ACKNOWLEDGMENT

It is impossible to thank everyone who had a part in the preparation of this report, but special recognition should be given to Mrs. Mary K. Wade, Mr. James W. Eng, and Mrs. Cora J. Cooper.

## DOCUMENT CONTROL DATA - R&amp;D

(Security classification of title, body of abstract and indexing annotation must be entered when the overall report is classified)

1. ORIGINATING ACTIVITY (Corporate author) U.S. Naval Research Laboratory Washington, D.C. 20390		2a. REPORT SECURITY CLASSIFICATION Unclassified	
		2b. GROUP	
3. REPORT TITLE TROPOSPHERIC RADIO DUCT METEOROLOGY AT VHF AND UHF IN THEORY AND AS OBSERVED ON A TRIP AROUND THE WORLD, FEBRUARY 8 TO MARCH 15, 1962			
4. DESCRIPTIVE NOTES (Type of report and inclusive dates) Interim report on the problem			
5. AUTHOR(S) (Last name, first name, initial) Randall, D.L.			
6. REPORT DATE May 31, 1966		7a. TOTAL NO. OF PAGES 84	7b. NO. OF REFS 19
8a. CONTRACT OR GRANT NO. NRL Problem R07-05		9a. ORIGINATOR'S REPORT NUMBER(S) NRL Report 6404	
b. PROJECT NO. RR 008-01-41-5553			
c.		9b. OTHER REPORT NO(S) (Any other numbers that may be assigned this report)	
d.			
10. AVAILABILITY/LIMITATION NOTICES Distribution of this document is unlimited.			
11. SUPPLEMENTARY NOTES		12. SPONSORING MILITARY ACTIVITY Dept. of the Navy (Office of Naval Research), Washington, D.C. 20360	
13. ABSTRACT Vorticity fields showing areas of divergence or convergence in the air-mass flow channels at or above the gradient wind level may be located on a weather map and are theoretically related to the formation or dissipation of elevated radio ducts at vhf and uhf. Theoretical predictions of elevated radio duct formation have been verified by measurements made on a trip around the world, February 8 to March 15, 1962, in a Naval Research Laboratory aircraft. It was verified that ducts result from warm dry air subsiding over cooler moist air in a divergence (anticyclone) area during conditions of stable or increasing pressure. On the basis of the theory and the meteorological measurements, oceanic regions in the world most likely to support radio duct formation at different seasons of the year were mapped. For either the Northern or the Southern Hemisphere, in winter these regions are predominantly in the Torrid Zone but in summer have extended farther into the Temperate Zone and are less prevalent in the Torrid Zone.			

14. KEY WORDS	LINK A		LINK B		LINK C	
	ROLE	WT	ROLE	WT	ROLE	WT
Radio transmission						
Radio reception						
Experimental data						
Theory						
Radio beams						
Atmosphere						
Troposphere						
Very high frequency						
Ultrahigh frequency						
Radio communication systems						
Air mass analysis						
Atmospheric motion, subsidence, lifting						
Temperature inversion						
Humidity						
Oceans						
Moisture gradient						

INSTRUCTIONS

1. **ORIGINATING ACTIVITY:** Enter the name and address of the contractor, subcontractor, grantee, Department of Defense activity or other organization (*corporate author*) issuing the report.

2a. **REPORT SECURITY CLASSIFICATION:** Enter the overall security classification of the report. Indicate whether "Restricted Data" is included. Marking is to be in accordance with appropriate security regulations.

2b. **GROUP:** Automatic downgrading is specified in DoD Directive 5200.10 and Armed Forces Industrial Manual. Enter the group number. Also, when applicable, show that optional markings have been used for Group 3 and Group 4 as authorized.

3. **REPORT TITLE:** Enter the complete report title in all capital letters. Titles in all cases should be unclassified. If a meaningful title cannot be selected without classification, show title classification in all capitals in parenthesis immediately following the title.

4. **DESCRIPTIVE NOTES:** If appropriate, enter the type of report, e.g., interim, progress, summary, annual, or final. Give the inclusive dates when a specific reporting period is covered.

5. **AUTHOR(S):** Enter the name(s) of author(s) as shown on or in the report. Enter last name, first name, middle initial. If military, show rank and branch of service. The name of the principal author is an absolute minimum requirement.

6. **REPORT DATE:** Enter the date of the report as day, month, year, or month, year. If more than one date appears on the report, use date of publication.

7a. **TOTAL NUMBER OF PAGES:** The total page count should follow normal pagination procedures, i.e., enter the number of pages containing information.

7b. **NUMBER OF REFERENCES:** Enter the total number of references cited in the report.

8a. **CONTRACT OR GRANT NUMBER:** If appropriate, enter the applicable number of the contract or grant under which the report was written.

8b, 8c, & 8d. **PROJECT NUMBER:** Enter the appropriate military department identification, such as project number, subproject number, system numbers, task number, etc.

9a. **ORIGINATOR'S REPORT NUMBER(S):** Enter the official report number by which the document will be identified and controlled by the originating activity. This number must be unique to this report.

9b. **OTHER REPORT NUMBER(S):** If the report has been assigned any other report numbers (*either by the originator or by the sponsor*), also enter this number(s).

10. **AVAILABILITY/LIMITATION NOTICES:** Enter any limitations on further dissemination of the report, other than those

imposed by security classification, using standard statements such as:

- (1) "Qualified requesters may obtain copies of this report from DDC."
- (2) "Foreign announcement and dissemination of this report by DDC is not authorized."
- (3) "U. S. Government agencies may obtain copies of this report directly from DDC. Other qualified DDC users shall request through \_\_\_\_\_."
- (4) "U. S. military agencies may obtain copies of this report directly from DDC. Other qualified users shall request through \_\_\_\_\_."
- (5) "All distribution of this report is controlled. Qualified DDC users shall request through \_\_\_\_\_."

If the report has been furnished to the Office of Technical Services, Department of Commerce, for sale to the public, indicate this fact and enter the price, if known.

11. **SUPPLEMENTARY NOTES:** Use for additional explanatory notes.

12. **SPONSORING MILITARY ACTIVITY:** Enter the name of the departmental project office or laboratory sponsoring (*paying for*) the research and development. Include address.

13. **ABSTRACT:** Enter an abstract giving a brief and factual summary of the document indicative of the report, even though it may also appear elsewhere in the body of the technical report. If additional space is required, a continuation sheet shall be attached.

It is highly desirable that the abstract of classified reports be unclassified. Each paragraph of the abstract shall end with an indication of the military security classification of the information in the paragraph, represented as (TS), (S), (C), or (U).

There is no limitation on the length of the abstract. However, the suggested length is from 150 to 225 words.

14. **KEY WORDS:** Key words are technically meaningful terms or short phrases that characterize a report and may be used as index entries for cataloging the report. Key words must be selected so that no security classification is required. Identifiers, such as equipment model designation, trade name, military project code name, geographic location, may be used as key words but will be followed by an indication of technical context. The assignment of links, roles, and weights is optional.